OPTIMAL DESIGN OF ELECTRIC BICYCLE

Yangbing Lou

Yuan Chang

Rongtao Jia

Hao Tan

ME 555-2011-03

Winter 2011 Final Report

4/22/2011

ABSTRACT

This project is on the design optimization of hybrid electric bicycle, which is a commercial product widely used in many parts of the world, such as China and India. This product has a very promising commercial potential. The customers always want to have a powerful and efficient hybrid electric bicycle. So, it will bring large profits if design optimization is done for these two aspects. This idea is the motivation for this project.The objective is to improve the performance of hybrid bicycle from the amount of power offered and efficiency of usage. There are four subsystems, which include Battery, Structure, Controller and DC motor. These subsystems have their individual objectives and constraints, and they interact with each other to optimize the final objective of the whole system. The anticipated results are expected as followed. First, the bicycle can achieve desired speed as high as possible. Second, the power is used with high efficiency. Third, every constraint is fulfilled when the objectives are optimal.

Table of Contents

1. INTRODUCTION

Electric-bicycle is a special type of bicycle with an electric motor on it. The motor provides additional riding power in addition to the human power. It also has a rechargeable battery to provide electric power to the motor and stores the mechanical from the human rider when motor is not in use. The advantage of this type of “hybrid” structure is that it reduces the human effort in riding and could be used for an extended range of distance, which is desired if the distance is relatively long compared with normal range. It also retains the desired characteristics of traditional bicycle. It has zero-emissions as it produces no combustion byproducts, which is environmentally friendly. It can also serves as a useful part of cardiac rehabilitation programs, since health professionals will often recommend a stationary bike be used in the early stages of these (wikipedia). The electric-bicycle is very popular in countries such as China, Demark, Netherlands and Australia. The power levels of motors used in the electric bicycles are influenced by available legal categories in these different countries (wikipedia).

Previous researchers have been making effort in the electric bicycle design. Annette Muetze and Ying Chin Tan from University of Wisconsin-Madison (wikipedia) used the modeling and simulation techniques to analyze the performance of DC-motor drive electric bicycle based on bicycle road test data. Their work focused on the controller design by using MATLAB/Simulink software, but it lacks of the detailed design of motor physical variables such as the sizing and weight, which is an essential problem in electric bicycle design but is hard to tackle due to the complexity of the bicycle system and the large amount of variables.

One way to approach the detailed electric bicycle design is the design optimization method. Julie Reyer and Panos Papalambros from University of Michigan Ann Arbor (Reyer, 2002) provides great insight in the motor design by using the design optimization method and pairs the motor system and motor controller systems together through a few common design variables. It also motivates us to utilize the design optimization approach to further analyze the application of DC-motor in electric bicycle system as well as other parts of electric bicycle.

In this project, the entire electric bicycle is divided into four subsystems: (1) Mechanical structure (2) Battery (3) DC-motor (4) Motor controller. The structure subsystem design aims to determine the optimal dimensions of the bicycle structure to achieve a minimal possible weight, while withstanding the loads and leaving enough space for battery and motor. The battery subsystem design aims to provide enough power input to the motor while targeting its minimum weight and maximum battery life during cyclic operation. The motor subsystem design aims to achieve the minimum possible weight of the motor while satisfying the power requirements. The motor controller design is trying to decide the controller gains that give rise to the minimum controller effort and desirable control specifications. Each subsystems will be designed individually among our team members and then integrated together to achieve the overall design objectives under the trade-offs between each subsystems.

The subsystem design task has been divided as follows:

Battery subsystem design – Yangbing Lou

DC-Motor subsystem design – Yuan Chang

Motor controller subsystem design – Rongtao Jia

Structure subsystem design – Hao Tan

2. SUBSYSTEM DESIGN

The entire electric bicycle is decomposed into four sub-systems and each team member is responsible for one individual system design optimization problem: (1) Battery system – Yangbing Lou, (2) DC motor system – Yuan Chang, (3) Motor controller design – Rongtao Jia, and (4) Structure system – Hao Tan.

Battery Subsystem Design – Yangbing Lou

2.1 Problem Statement

Battery is a very important subsystem to offer the power which motivates the bicycle motor. In addition, more efficiently using the energy inside a battery is becoming increasing important in energy field. Battery's weight, working temperature, energy efficiency and capacity are the main concerns in this project. Li-ion battery is chosen for this project since apart from a high specific energy, it also has considerable low self-discharge rate, and is more capable for high current and voltage output (Henk, 2002).

In general, for the same type of battery, the more energy it stores, the more weight it has and simultaneously, the more volume it occupies. Though the battery with more energy has a longer working cycle, it requires extra weight for more cells (Henk 2002)to supply power actuating the bicycle at the same speed, comparing to the bicycle with less weight. It is desired that the battery should work longer and more efficiently. Under this constraint and based on the road conditions, riders' using habit, the corresponding optimization design could be determined.

Furthermore, it is concluded that the temperature of battery depends on the current output, and working time, which will directly determine the power of motor and the speed of electric bicycle. The temperature of the battery will have a significant effect on battery's performance, such as energy efficiency and capacity. Typically, the operating temperature range for Li-ion battery is -20 to 50 ^{o}C (G.H. Kim, [2006]). Higher power output of battery will lead to higher bicycle speed, while increase the temperature of battery and reduce the battery's efficiency. Considering the tradeoff between these two, the corresponding relation and equations can be derived to solve the optimization problem.

In real case, these are more issues needed to be considered for the battery system, such as cell balancing, state of charge estimation, prevention of over-discharging, battery's life cycle consideration. However, to understand the simple behavior of Li-ion battery affected by temperature, the model that will be built has the following assumptions. At first, the battery used is fresh, which means there is no aging process and no energy self-discharge. Also, the electrical energy remaining in each battery cell should be the same, which means the cells should have the same performance all the time. Furthermore, the battery should have small current output since the properties of Li-ion battery will not only be affected by temperature, but also high current output. At low current, the performance of battery is dominated by temperature. Above all, the battery model in this project is used to analyze the Li-ion battery behavior affected by temperature, and is used to find the optimal solution when the battery works with higher energy efficiency, high energy stored in the battery cell, as well as small number of battery cells.

Previous team Piyush Soni, Sha Li from ME555, winter 2009 has designed a battery model for electric bicycles, with Li-ion battery. They emphasized design variables and problem on the inner structure of battery, such as the resistance, thickness of electrodes, separators, current collectors, and active material properties (e.g. conductivity). Temperature was considered but not related to the battery's performance.

2.2 Nomenclature

All symbols used are given below, with units for each quantity.

Symbol	Units	Definition
C_c	Ah	Battery capacity
C_{bat}	Wh/kg	Specific weight energy
C_{ll}	wh/kg	Capacity lower limit
C_{ul}	wh/kg	Capacity upper limit
C_{ct}	Ah	Battery total capacity
H_{bat}	h	Battery inductance
I_{bat}	A	Battery output current
I_{ll}	A	Battery current lower limit
I_{ul}	A	Battery current up limit
n_{cel}	na	Number of cells
n_{lim}		Limit for number of cells
R_{cell}	Ω	Battery cell resistance
R_{bat}	Ω	Total battery resistance
T_{bat}	^oC	Battery temperature
T_{env}	^oC	Environmental temperature
T_{max}	^oC	Maximum battery temperature
T_{min}	^oC	Minimum battery temperature
V_{bat}	V	Battery output voltage
V_{bic}	km/h	Bicycle speed
V_{ll}	V	Battery lower voltage limit
V_{lim}	km/h	speed limit
V_{ul}	m^3	battery upper voltage limit
V_{oc}	V	Battery open circuit voltage
W_{bat}	kg	Battery total weight
W_{cel}	kg	weight per cell
W_{lim}	kg	weight constraint for battery
η_{bat}	%	Energy's efficiency

2.3 Mathematical Model

Objective function

The objective of the battery subsystem is to maximize the battery capacity, cycle life, and minimize the battery mass to have the optimal traveling distance for an electric bicycle.

Object function: min $\frac{W_{bat}}{C_{ca} \times \eta_{bat}}$

Constraints

Each constraint is described below.

Physical Constraints

Temperature constraint: the working temperature for Li-ion battery is 20 to 50 ^{o}C. In addition, the temperature of battery is a function of number of cells, working time, output current, out voltage, and environmental temperatures.

$T_{bat} – T_{max} \leq 0$

$T_{min} – T_{bat} \leq 0$

$h(T_{bat}, R_{cell}, C_c) = 0$

Current & voltage output constraint: Li-ion battery cell has current output limit. It is also a variable depending on inner resistance, load resistance, load back emf. In this project, we assume the cell open circuit voltage keeps constant.

$I_{bat} – I_{ul} \leq 0$

$I_{ll} – I_{bat} \leq 0$

$V_{ll} – V_{bat} \leq 0$

$V_{bat} – V_{ul} \leq 0$

$h(R_{cell}, T_{bat}) = 0$

$Vbat = n_{cell} *(V_{oc} – I_{bat} * R_{cell})$

Capacity constraint of each cell: the battery capacity will decrease during its cycle life. We assume every time the battery is used, it is at fully charged conditions. It is a function of cycle life, and discharge rate. However, in this project, only fresh battery is considered.

$C_{ct} – n * C_c = 0$

$C_c – C_{ul} \le 0$

$C_{ll} – C_c \le 0$

$h(C_{bat}, T_{bat}) = 0$

Practical Constraints

Speed limit set by law: In china, the speed limit for electric bicycle is 20 km/h. the speed of bicycle is a function of battery current, voltage, resistance, and other bicycle properties.

$V_{bic} – V_{lim} \le 0$

$h(V_{bic}, I_{bat}, V_{bat}, R_{bat}) = 0$

Weight constraint: although it is the design variable in the battery subsystem, limit still exists due to the structure material properties, bicycle control consideration and ergonomic.

$W_{bat} – W_{lim} \le 0$

$W_{bat} – n_{cel} \times W_{cel} = 0$

Energy efficiency constraint: the energy efficiency of a battery should be around 70% - 100%, which is appropriate for energy’s utilization.

$\eta_{bat} – 100\% \le 0$

$70\% – \eta_{bat} \le 0$

$\eta_{bat} = 1– I_{bat}R_{cel}/V_{oc}$

Design variables and parameters

The design variables, as well as a set of typical values in an application, which is a feasible solution in the battery model Currie Technologies Rack Mount Battery for E-Zip Electric Bikes, Model# SLA Rack Mount Battery, are shown below.

Table 1. Design variables of battery subsystem

Symbol	Units	Definition	Feasible value
C_{bat}	Ah	Capacity	12
η_{bat}	%	Energy efficiency	90%
W_{bat}	kg	Battery total weight	6.9

Table 2. Parameters of battery subsystem

Symbol	Units	Definition	Value
C_{lim}	wh/kg	capacity limit	280
D_{bat}	wh/l	specific volume energy	115
I_{ul}	A	battery current up limit	10
n_{lim}		limit for number of cells	14
R_{bat}	Ω	battery total resistance	0.3
T_{env}	ºC	environmental temperature	23
T_{max}	ºC	maximum battery temperature	50
T_{min}	ºC	minimum battery temperature	-20
V_{bat}	V	Battery output voltage	3.6
V_{lim}	km/h	speed limit	20
W_{cel}	kg	weight per cell	0.3
W_{lim}	kg	weight constraint for battery	10

Summary model

The summary of the entire battery subsystem's optimization problem is shown below, with the primary objective function and all the constraints in standard form.

Objective function: min f = $\frac{W_{bat}}{C_{bat} \times \eta_{bat}}$

Subjected to:

g1: $T_{bat} - T_{max} \leq 0$

g2: $T_{min} - T_{bat} \leq 0$

g3: $I_{bat} - I_{ul} \leq 0$

g4: $I_{ll} - I_{bat} \leq 0$

g5: $V_{ll} - V_{bat} \leq 0$

g6: $V_{bat} - V_{ul} \leq 0$

g7: $C_{ca} - C_{lim} \leq 0$

g8: $n_{cel} - n_{lim} \leq 0$

g9: $V_{bic} - V_{lim} \leq 0$

g10: $W_{bat} - W_{lim} \leq 0$

h1: $W_{bat} - n_{cel} \times W_{cel} = 0$

h2: $h(T_{bat}, R_{cell}, C_c) = 0$

h3: $V_{bat} - n_{cell} * (V_{oc} - I_{bat} \times R_{cell}) = 0$

h4: $h(R_{cell}, T_{bat}) = 0$

h5: $C_{bat} - n * C_{cel} = 0$

h6: $E_{bat} - E_{load} + I_{bat} \times (R_{bat} + R_{load}) = 0$

h7: $P_{bat} - I_{bat} \times V_{bat} = 0$

h8: $h(T_{bat}, I_{bat}, V_{bat}, T_{env}, n_{cel}) = 0$

h9: $\eta_{bat} - (1 - I_{bat} R_{cel} / V_{oc}) = 0$

The constraint equations h2, h4 are determined by curve-fitting methods using the data from database (G.H. Kim and A. Pesaran, 2002). The results are shown in the next page.

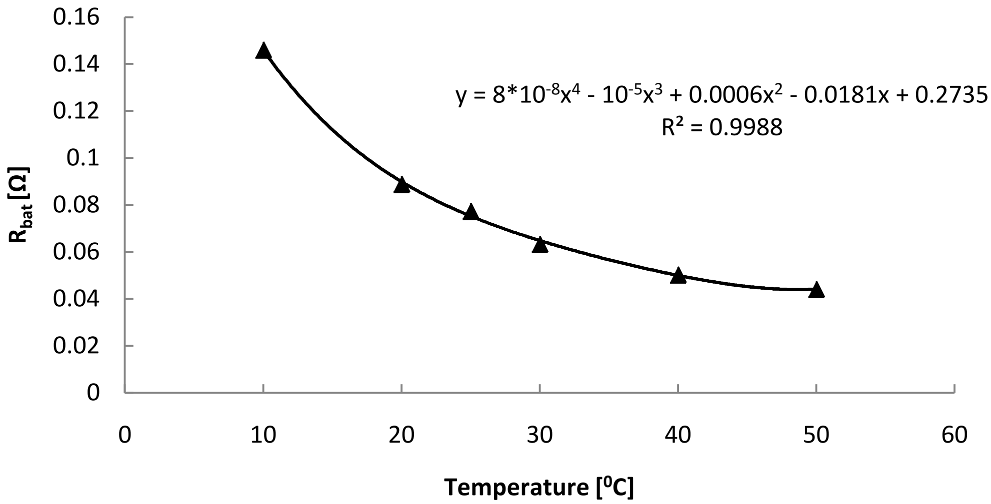

Figure 2.3.1. Relation between cell resistance and temperature by using polynomial curve fitting, with R^2 = 0.9988

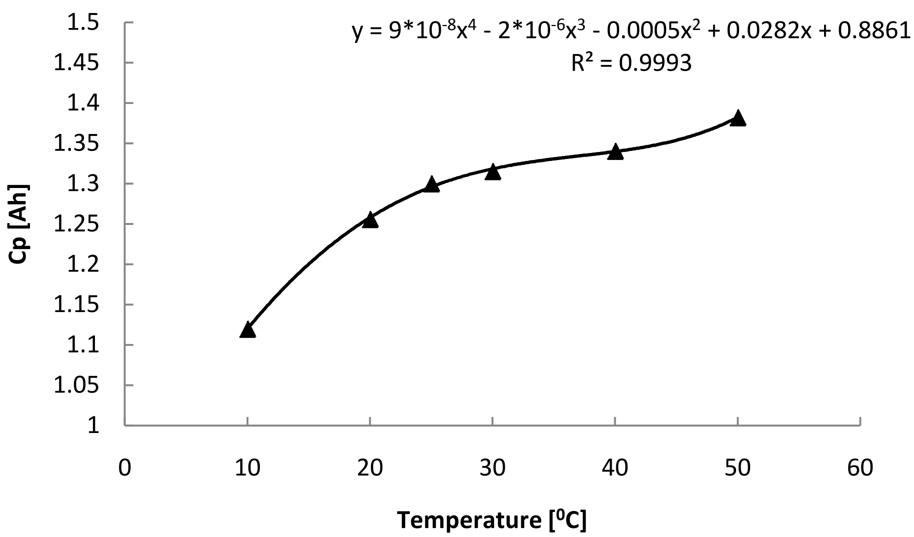

Figure 2.3.2. Relation between cell capacity and temperature by using polynomial curve fitting, with R^2 = 0.9993

Above all, this mathematical model is valid to be used for optimization when the temperature of battery is controllable and will varies from 10 to 50 °C. In addition, the current of the battery shouldn't be higher than 1 A since the too fitting curves are only valid at low current.

By setting the value for the parameters and using equation simplification and the relation determined by curve fitting, the complete and validated mathematical model is shown below, where T is the battery temperature, which is the same as T_{bat}, previously been denoted. In addition, the obvious inactive constraints have been removed in the model.

Objective function: f =

$$\frac{0.3\times n_{cell}}{(9\times10^{-8}T^4 - 2\times10^{-6}T^3 - 0.0005T^2 + 0.0282T + 0.8861)\times[1 - \frac{I_{bat}(8*10^{-8}T^4 - 10^{-5}T^3 + 0.0006T^2 - 0.0181T + 0.2735)}{3.6}]}$$

Subjected to:

g1: $T - 50 \le 0$

g2: $10 - T \le 0$

g3: $I_{bat} - 10 \le 0$

g4: $0.1 - I_{bat} \le 0$

g5: $13 - n_{cell} *(3.6 - I_{bat} \times (8 * 10^{-8}T^4 - 10^{-5}T^3 + 0.0006T^2 - 0.0181T + 0.2735)) \le 0$

g6: $n_{cell} *(3.6 - I_{bat} \times (8 * 10^{-8}T^4 - 10^{-5}T^3 + 0.0006T^2 - 0.0181T + 0.2735)) - 50 \le 0$

g7: $(9 \times 10^{-8}T^4 - 2 \times 10^{-6}T^3 - 0.0005T^2 + 0.0282T + 0.8861) - 1.5 \le 0$

g8: $1.1 - (9 \times 10^{-8}T^4 - 2 \times 10^{-6}T^3 - 0.0005T^2 + 0.0282T + 0.8861) \le 0$

g9: $(9 \times 10^{-8}T^4 - 2 \times 10^{-6}T^3 - 0.0005T^2 + 0.0282T + 0.8861) * n_{cell} - 40 \le 0$

g10: $1.1 - (9 \times 10^{-8}T^4 - 2 \times 10^{-6}T^3 - 0.0005T^2 + 0.0282T + 0.8861) * n_{cell} \le 0$

g11: $n_{cel} - 15 \le 0$

g12: $0 - n_{cel} \le 0$

The degree of freedom for this model is three, which is described the three design variables, T_{bat}, I_{bat} and n_{cell}.

2.4 Model Analysis

In this section, the monotonicity principles are used to analyze and simplify the model.

Monotonicity analysis

Table 1. The monotonocity table

	n_{cell}	I_{bat}	T
f	+	+	U
g1			-
g2			+
g3		+	
g4		-	
g5	-	+	-
g6	+	-	+
g7			+
g8			-
g9			+
g10			-
g11	+		
g12	-		

The monotonicity table of the model in previous page is shown above. After checking all the constraints and the objective function, the optimization problem is well bounded. Then the monotonicity analysis was applied to solve the problem by using First (MP1) and Second (MP2) Monotonicity Principles.

Step 1: Considering the variable n_{cell}, by MP1, g5 or g12 must be active. If g12 is active, which means n is equal to 0, g5 ($13 \le 0$) is not satisfied. Hence, g5 must be active and one equality constraint between variables from g3 can be determined as follows.

$$n_{cell} = \frac{13}{3.6 - \mathrm{I_{bat}}\ \mathrm{x}\ (8 * 10^{-8}\mathrm{T}^4\ -\ 10^{-5}\mathrm{T}^3\ +\ 0.0006\mathrm{T}^2\ -\ 0.0181\mathrm{T}\ +\ 0.2735)}$$

Then the mathematical model will be simplified to as follows.

$$\text{Min } f= \frac{\frac{3.9}{3.6 - I_{bat} \times (8*10^{-8}T^4 - 10^{-5}T^3 + 0.0006T^2 - 0.0181T + 0.2735)}}{(9\times10^{-8}T^4 - 2\times10^{-6}T^3 - 0.0005T^2 + 0.0282T + 0.8861)\times[1 - \frac{I_{bat}(8*10^{-8}T^4 - 10^{-5}T^3 + 0.0006T^2 - 0.0181T + 0.2735)}{3.6}]}$$

Subjected to:

g1: $T - 50 \leq 0$

g2: $10 - T \leq 0$

g3: $I_{bat} - 10 \leq 0$

g4: $0.1 - I_{bat} \leq 0$

g5: $(9 \times 10^{-8}T^4 - 2 \times 10^{-6}T^3 - 0.0005T^2 + 0.0282T + 0.8861) - 1.5 \leq 0$

g6: $1.1 - (9 \times 10^{-8}T^4 - 2 \times 10^{-6}T^3 - 0.0005T^2 + 0.0282T + 0.8861) \leq 0$

g7: $\frac{(9\times10^{-8}T^4 - 2\times10^{-6}T^3 - 0.0005T^2 + 0.0282T + 0.8861)*13}{3.6 - I_{bat} \times (8*10^{-8}T^4 - 10^{-5}T^3 + 0.0006T^2 - 0.0181T + 0.2735)} - 40 \leq 0$

g8: $1.1 - \frac{(9\times10^{-8}T^4 - 2\times10^{-6}T^3 - 0.0005T^2 + 0.0282T + 0.8861)*13}{3.6 - I_{bat} \times (8*10^{-8}T^4 - 10^{-5}T^3 + 0.0006T^2 - 0.0181T + 0.2735)} \leq 0$

g9: $\frac{13}{3.6 - I_{bat} \times (8*10^{-8}T^4 - 10^{-5}T^3 + 0.0006T^2 - 0.0181T + 0.2735)} - 15 \leq 0$

The monotonicity table of simplified model is shown below.

Table 2. The monotonicity table of simplified model for step 1

	I_{bat}	T
f	+	U
g1		-
g2		+
g3	+	
g4	-	
g5		+
g6		-
g7	+	U
g8	-	U
g9	+	-

Step 2:

Considering the variable I_{bat}, by MP1, g4 or g8 in Table 2 must be active. If g4 is active, I_{bat} = 0.1. The problem can be simplified as follows:

At this point, it is still hard to determine the monotonicity of the objective function and hence, other methods should be applied to solve the optimization problem.

$$\text{Min } f = \frac{\frac{3.9}{3.6 - 0.1(8*10^{-8}T^4 - 10^{-5}T^3 + 0.0006T^2 - 0.0181T + 0.2735)}}{(9\times10^{-8}T^4 - 2\times10^{-6}T^3 - 0.0005T^2 + 0.0282T + 0.8861)\times[1 - \frac{0.1(8*10^{-8}T^4 - 10^{-5}T^3 + 0.0006T^2 - 0.0181T + 0.2735)}{3.6}]}$$

Subjected to:

g1: $T - 50 \le 0$

g2: $10 - T \le 0$

g3: $9 \times 10^{-8}T^4 - 2 \times 10^{-6}T^3 - 0.0005T^2 + 0.0282T - 0.6139 \le 0$

g4: $-9 \times 10^{-8}T^4 + 2 \times 10^{-6}T^3 + 0.0005T^2 - 0.0282T + 0.2139 \le 0$

g5: $9.64 \times 10^{-8}T^4 - 2.8 \times 10^{-6}T^3 - 4.52 \times 10^{-4}T^2 + 0.0268T - 1.972 \le 0$

g6: $-9.88 \times 10^{-8}T^4 + 3.1 \times 10^{-6}T^3 + 4.34 \times 10^{-4}T^2 - 0.0262T + 3.044 \le 0$

g7: $8 \times 10^{-8}T^4 - 10^{-5}T^3 + 0.0006T^2 - 0.0181T + 0.2468 - 3.387 \le 0$

At this point, it is hard to determine the monotonicity of the objective function and hence, optimum packages will be applied to solve the problem. Excel solver, and MATLAB *fmincon* will be used to solve the problem and check the availability of the solution.

Step 3:

Then if g8 in Table 2 is active, the equality constraint can be determined from g8, which is shown below.

$$1.1 = \frac{(9 \times 10^{-8}T^4 - 2 \times 10^{-6}T^3 - 0.0005T^2 + 0.0282T + 0.8861) * 13}{3.6 - I_{bat} \text{ x } (8 * 10^{-8}T^4 - 10^{-5}T^3 + 0.0006T^2 - 0.0181T + 0.2735)}$$

Furthermore the model can be simplified to as follows.

$$\text{Min } f = \frac{16.988}{(9\times10^{-8}T^4 - 2\times10^{-6}T^3 - 0.0005T^2 + 0.0282T + 0.8861)^3}$$

Subjected to:

g1: $T - 50 \le 0$

g2: $10 - T \le 0$

g3: $9 \times 10^{-8}T^4 - 2 \times 10^{-6}T^3 - 0.0005T^2 + 0.0282T - 0.6139 \le 0$

g4: $-9 \times 10^{-8}T^4 + 2 \times 10^{-6}T^3 + 0.0005T^2 - 0.0282T + 0.2139 \le 0$

g5: $9.125 * 10^{-8}T^4 - 1.0125 \times 10^{-5}T^3 + 5.275 \times 10^{-4}T^2 - 0.014575T + 0.0243 \le 0$

At this point, it is also hard to determine the monotonicity of the constraints by hand calculation and hence, optimum packages will be applied to solve the problem.

Step 4

After using Excel solver for the model in step 2 and 3, it is determined that when current, I_{bat}, is equal to 0.1, the minimum value of the objective function is smaller than that in step 3, when g8 in step 1 is active. The result is shown below.

Table 3. Activity of constraint g4 and g8

	Objective function	T_{bat}
g8 active	1.173	34.9
g4 active	0.821	50

Above all, based on the monotonicity analysis, it can be concluded that g4, and g5 of original model should be active when considering the variable n_{cell} and I_{bat}. These two active constraints can generate two equality constraints and the original model can be simplified with only one degree of freedom. Further computation is required to determine temperature behavior of the original model.

2.5 Optimization Study

Excel solver with Generalized Reduced Gradient method was used to solve the problem of original model and simplified model. MATLAB fmincon function with SQP methods was also used to solve the simplified model to check the availability of final results.

From excel solver, the minimum value of the non-simplified and simplified objective function are both 0.821, while the current I_{bat} is equal to 0.1, and the temperature is equal to 50. From MATLAB fmincon function, the minimum value of the model is also 0.821. The results are shown below.

Table 4. Optimal solution of non-simplified model by Excel Solver

	Objective function	T_{bat}	I_{bat}	n_{cell}
Initial value	0.730	20	0.2	3
Final solution	0.821	50	0.1	3.66

Table 5. Optimal solution of simplified model by Excel Solver

	Objective function	T_{bat}
Initial value	0.730	20
Final solution	0.821	50

Table 6. Optimal solution of simplified model by MATLAB fmincon

	Objective function	T_{bat}
Initial value	0.730	20
Final solution	0.821	50

Since the number of battery cells should be integer, the solution is then modified to n_{cell} = 4. And when n is equal to 3, the constraint g5 cannot be satisfied. After comparing the results computed from MATLAB and EXCEL solver, there is no difference observed until the results count to 10^{-5}. Due to the different small step size for both methods, the difference exists but is insignificant. It is also observed that the solution is a boundary solution, which is not an interior solution. This is because the optimum point is found at the boundary of the constraints g1, g4, and g5. Due to the physical properties of battery, the range of the constraints cannot be extended. For instance, the temperature of the battery could not be higher than 50 °C, lower than 10 °C in order to have good performance. Furthermore, the minimum current required to motivate the motor and the maximum current that will not burn the motor also determine the constraints in the model. If other type of Li-ion battery is developed, they constraints can be changed and the interior solution may be found.

Furthermore, the sensitivity report was generated by EXCEL to check the activity of each constraint, which is shown below.

Table 7. Sensitivity result

Constraint	Final Value	Lagrange Multiplier
g1	0	-0.00426
g2	-40	0
g3	-9.9	0
g4	0	-0.234
g5	$1.27*10^{-7}$	-0.0631
g6	-37.0	0
g7	-0.141	0
g8	-0.259	0
g9	-35.0	0
g10	-3.88	0
g11	-11.3	0
g12	-3.66	0

The Lagrange Multipliers in above table show that constraints g1, g4, and g5 are active. Due to the computational algorithm in EXCEL Solver, the final value of g5 is not equal to 0. However, it is infinitesimal and can be considered as 0. This means g5 is active, which can be proved by the nonnegative value of Lagrange Multiplier. In addition, these negative multipliers of g1, g4, and g5 agree with the results analyzed by monotonicity analysis. Since EXCEL Solver should use positive null form to solve the problem, the Lagrange Multipliers are negative, not positive in the KKT conditions for negative null form.

KKT conditions

For the simplified model, there is no equality constraint and hence the multipliers λ for equality constraints are zero. The necessary conditions for the optimization problem, known as the Karush-Kuhn-Tucker (KKT) conditions are shown below.

$$\nabla f_* + \boldsymbol{\mu}^T \nabla \boldsymbol{g}_* = \mathbf{0}^T$$

Where μ ≥ 0 for negative null form, and $\boldsymbol{\mu}^T \nabla \boldsymbol{g} = \mathbf{0}.$ Using the simplified model, the KKT conditions are determined, which is shown below.

$$\nabla f_* = \frac{-50.96 \times (3.6 \times 10^{-7}\mathrm{T}^3 - 6 \times 10^{-6}\mathrm{T}^2 - 0.001\mathrm{T} + 0.0282)}{(9 \times 10^{-8}\mathrm{T}^4 - 2 \times 10^{-6}\mathrm{T}^3 - 0.0005\mathrm{T}^2 + 0.0282\mathrm{T} + 0.8861)^4}$$

$$\boldsymbol{\mu}^T \nabla \boldsymbol{g}_* = \mu_1 - \mu_2 + \mu_3(3.6 \times 10^{-7}\mathrm{T}^3 - 6 \times 10^{-6}\mathrm{T}^2 - 0.001\mathrm{T} + 0.282)$$
$$+\mu_4(-3.6 \times 10^{-7}\mathrm{T}^3 + 6 \times 10^{-6}\mathrm{T}^2 + 0.001\mathrm{T})$$
$$+\mu_5(3.65 \times 10^{-7}\mathrm{T}^3 - 3.0375 \times 10^{-5}\mathrm{T}^2 + 1.055 \times 10^{-3}\mathrm{T} - 0.01458)$$

KKT conditions:

$$\nabla f_* + \boldsymbol{\mu}^T \nabla \boldsymbol{g}_* = \mathbf{0}^T$$
$$\mu_1(T - 50) = 0$$
$$\mu_2(T - 10) = 0$$
$$\mu_3(9 \times 10^{-8}\mathrm{T}^4 - 2 \times 10^{-6}\mathrm{T}^3 - 0.0005\mathrm{T}^2 + 0.0282\mathrm{T} - 0.6139) = 0$$
$$\mu_4(-9 \times 10^{-8}\mathrm{T}^4 + 2 \times 10^{-6}\mathrm{T}^3 + 0.0005\mathrm{T}^2 - 0.0282\mathrm{T} + 0.2139) = 0$$
$$\mu_5(9.125 \times 10^{-8}\mathrm{T}^4 - 1.0125 \times 10^{-5}\mathrm{T}^3 + 5.275 \times 10^{-4}\mathrm{T}^2 - 0.014575\mathrm{T} + 0.0243) = 0$$
$$\boldsymbol{g} \leq \mathbf{0}$$

The real solution for equation

$$(9 \times 10^{-8}\mathrm{T}^4 - 2 \times 10^{-6}\mathrm{T}^3 - 0.0005\mathrm{T}^2 + 0.0282\mathrm{T} - 0.6139) = 0$$

are 59.5 and -89.1; while the real solution for equation

$$(9.125 \times 10^{-8}\mathrm{T}^4 - 1.0125 \times 10^{-5}\mathrm{T}^3 + 5.275 \times 10^{-4}\mathrm{T}^2 - 0.014575\mathrm{T} + 0.0243) = 0$$

are 57.3 and 1.78. None of the solution satisfies the first and second constraints. Hence, μ_3, μ_4, and μ_5 are equal to 0. Using the case by case examination, the possible solutions are solved as follows.

$$T = 50$$

$$\mu_1 = 0.123$$
$$\mu_2 = 0$$
$$\mu_3 = 0$$
$$\mu_4 = 0$$
$$\mu_5 = 0$$

The nonzero multiplier of the first constraint agrees with what is determined from EXCEL solver. The constraint g1: $T - 50$ is active for non-simplified model solved by EXCEL Solver and the simplified model solved by KKT conditions. Since the model is different and the constraints are changed, the value of multiplier is different. It verifies that the results are correct and the methods are valid.

Global and local optimal point

To check whether the point found previously is the global solution, several initial points were used for the non-simplified model and the results are shown below. All the results are the same until the optimal value counts to 10^{-7}. It means the solution (T_{bat}, I_{bat}, n_{cell}) = (50, 0.1, 4) are the global solution for this model. The small difference exist is because of the step size and the value of ε in the computational algorithm.

Table 8. Optimal value of objective function by using different initial points

T_{bat}	I_{bat}	n_{cell}	Objective Function
50	0.1	3	0.820864652
40	0.5	7	0.820864665
30	0.7	10	0.820864680
40	0.1	1	0.820864747
10	0.2	3	0.820864728

2.6 Parametric Study

The parameters studied here are the battery's open circuit voltage, V_{oc}, battery's weight per cell, W_{cel}, and the coefficients for C_p and R_{bat}. To check the sensitivity, one parameter was changed by percentage while other parameters and design variable are fixed at the optimal points. The results are shown below.

Table 9. Parametric studies

At optimal point	w_{cell}		V_{oc}		C_p		R_{bat}	
Change of parameter	+20%	-20%	+20%	-20%	+20%	-20%	+20%	-20%
Change of objective function	+20%	-20%	-17.1%	+25.9%	-16.7%	+25%	0.58%	-0.57%

Among these parameters, R_{bat} is the most insensitive parameter since when the coefficient of R_{bat} changes by 20 percent, the change of objective function is less than 1 %. The objective function is sensitive for parameter W_{cell}, V_{oc} and C_p but it is hard to distinguish the difference among them. When the design variables are at other feasible points, the results are similar and hence, it is concluded that the change of battery's inner resistance will have smaller effect on the system than other parameters.

2.7 Discussion of Results

The final results determined for the battery model are

$$I_{bat} = 0.1 \text{ A},$$

$$T_{bat} = 50\ ^{0}\text{C},$$

$$N_{cell} = 4.$$

The total mass of the battery is 1.2 kg and the energy efficiency is about 99.8%. It can be observed that the battery should work at low current and high temperature, with 4 battery cells to provide the required voltage. The low current follows the rule since the inner resistance of the battery will consume small energy with low current. The less the energy consumed, the higher the energy efficiency will be. Furthermore, when the working temperature is high, the battery can release more energy due to the completed chemical reactions and Lithium ion movement. This can results in a high battery capacity. Hence, regardless of electric bicycle's moving speed and battery's life cycle, a bicycle can run further by the same amount of energy with lower current and higher temperature. To have long mileage, an electric bicycle can have multiple battery cells and 4 of them can be used at the same time. After the 4 cells dissipate all energy, the battery can switch to another package with 4 cells and continues to work. These criteria can work for design optimization problems of any type of electric bicycle with Li-ion batteries. However, it has several limitations.

The model only considers the new battery's behavior at low current. The inner resistance and other battery properties will be affected by high current output. Hence, the model is not valid for high current. And for different kinds of battery, the current constraints will vary and result in different optimal solutions. On the other hand, when the ageing process happens, the battery model will no longer be valid due to the significant change of inner resistance and capacity. Furthermore, when battery works at high temperature, it can release more energy in one cycle but the total cycle life will reduces. The problem will be more challenge and significant if a complete and complex battery model is considered. It should be insured that a battery should work at high energy efficiency as well as long cycle life.

DC-Motor Subsystem Design – Yuan Chang

2.1 Problem Statement

An important feature of electric bicycle is that it has a motor-driven regime, while the traditional bicycle does not have this electromechanical component. Therefore, the motor design plays an essential role in the overall design optimization problem of the entire system. In this project, a brushed type dc-motor is considered. Its application in the electric bicycles has been shown to exist and has drawn attention from previous researchers (Annette, 2007).

The brushed type dc-motor takes the voltage in the armature as an input. The armature circuit is composed of a resistance and inductance, which causes a changing value of current in the armature. This current generates a magnetic field around the armature, thus causing the commutator to rotate.

The design objective is to achieve the minimum possible weight of the motor. To achieve this goal, several variables need to be designed carefully. These variables including the rotor diameter, depth of slots, rotor axial length, length of armature wire and length of field wire. One trade-off in this design is that as the length of armature wire and field wire increase, the magnetic field becomes stronger. However, this also increases the space it occupied and put on more weight to the motor. These variables also determine the important constant for motor dynamic behavior, such as the motor constant, resistant and inductance. Therefore, the design optimization approach is needed to ensure that these variables are chosen to achieve the objectives while satisfying all the constraints at the same time. The entire model is based on previous research by (Julie, 2002). In this model, several design criteria were carefully examined, such as the specific electric loading, the permissible heat loss, and other geometric considerations. The following subsections will give a detailed explanation about this model and its application in order to solve the DC-motor subsystem design optimization problem.

2.2 Nomenclature

Symbols	Description	Units
a	Number of parallel paths	1
A_{wa}	Cross-section area of armature wire	m^2
A_{wf}	Cross-section area of field wire	m^2
ac	Specific electrical loading	kA/m
b_{fc}	Depth of field coil	m
D	Rotor diameter	m
d_s	Depth of slots	m
f_{cf}	Copper space factor	1
h_f	Height of field windings	m
I_f	Field current	A
L	Rotor axial length	m
L_{mtf}	Mean turn length of field coil	m
L_{wa}	Length of armature wire	m
L_{wf}	Length of field wire	m
n_d	Rotational speed	rad/s
p	Number of poles	1
P_{mind}	Minimum required power	kW
S	Number of slots or teeth on rotor	1
η	Motor efficiency	1
ρ_{Cu}	Density of copper	kg/m^3
ρ_{Fe}	Density of iron	kg/m^3
ψ	Pole arc to pole pitch ratio	1

2.3 Mathematical Model

This section provides a detailed description of the mathematical model of motor subsystem. This model translates the engineering problem into a mathematical form which will be used later to perform the design optimization study. This section have five parts: (1) Objective function, (2) Constraints, (3) Design variables and parameters, (4) Initial model before simplification, and (5) Summary model

Objective function

The objective is to minimize the weight of the motor. The entire model was fully developed in (Julie, 2002). The objective function is defined as:

$$\text{Minimize } W = \rho_{Cu}(A_{wa}L_{wa} + A_{wf}L_{wf}) + \rho_{Fe}L\pi(D + d_s)^2$$

Here, W represents the total weight of the motor, which is comprised of two parts: (1) copper wires of armature and field circuits, and (2) rotor body made of iron. The weight of stator body is not included in the objective function since it is assumed constant in this application and not changing with the design problem. As indicated in the objective function, there are five design variables: L_{wa}, L_{wf}, L, D, d_s. The values for these variables are chosen based on the physical limitations as well as the constraints from this particular application.

Constraints

One design interest is the specific electrical loading ac, which is defined as the number of armature (or stator) ampere conductors per meter of armature (or stator) periphery at the air-gap (kA/m). Its expression is given in (Julie, 2002) as:

$$ac = \frac{2P_{\min_d}L_{wa}}{\pi\eta a n_d(2L + \frac{2.3\pi D}{p} + 5d_s)D}$$

As shown in the equation, the specific electrical loading is a function of the design variables (L_{wa}, L, D, d_s). All the other quantities appeared in the equation are assumed constant in this application and serve as design parameters. It should be noted here that the minimum required power (P_{mind}) and the rotational speed (n_d) are variables in the motor controller subsystem, but are considered as parameters in this subsystem. They will be designed carefully when the subsystems are integrated together. It is given a lower bound and upper bound as:

$$6 \le ac \le 20$$

Another design interest is the field current, which is defined as:

$$I_f = \frac{A_{wf}^2 n_d}{h_f L_{mtf} b_{fc} f_{cf} p \rho}$$

The mean turn length (L_{mtf}) and height of field windings (h_f) in the above equation are defined as:

$$L_{mtf} = L + 2b_{fc}$$
$$h_f = \frac{0.076\psi}{L}$$

The field current is limited by the permissible heat loss per unit of surface area (W/m^2):

$$150 \le \frac{(10I_f)^2 L_{wf} \rho}{A_{wf}(L_{mtf} + b_{fc})h_f} \le 750$$

There are also some constraints from geometric and spacing requirements. For example, the spacing between stator and rotor should be large enough for the winding wires. This constraint is expressed as:

$$\frac{1.2L_{wa}A_{wa}}{2L+\frac{2.3\pi D}{p}+5d_s} \le \pi[(\frac{D}{2})^2-(\frac{D}{2}-d_s)^2]$$

Other geometric constraints are summarized in detail in the *Summary model* section. It should be noted here that the bounds for these constraints are determined based on the nominal values in previous literature (Julie, 2002) and are modified to satisfy the specific requirements from electric bicycle application.

Design variables and parameters

The design variables and parameters for the motor subsystem are summarized below:

Variables: L_{wa}, L_{wf}, L, D, d_s

Parameters: a, A_{wa}, A_{wf}, b_{fc}, f_{cf}, n_d, P_{mind}, p, S, η, ρ, ρ_{Cu}, ρ_{Fe}, ψ

Table 2.3.1 and 2.3.2 below provide a full list of design variables and design parameters. The values for the parameters are based on the general design guidelines in (Hamdi, 1994) as well as the limitations of the electrical bicycle application.

Table 2.3.1: List of design variables

Symbols	Description	Units
L_{wa}	Length of armature wire	m
L_{wf}	Length of field wire	m
L	Rotor axial length	m
D	Rotor diameter	m
d_s	Depth of slots	m

Table 2.3.2: List of design parameters

Symbols	Description	Values	Units
a	Number of parallel paths	5	1
A_{wa}	Cross-section area of armature wire	2×10^{-6}	m^2
A_{wf}	Cross-section area of field wire	1×10^{-6}	m^2
b_{fc}	Depth of field coil	0.045	m
f_{cf}	Copper space factor	0.65	1
n_d	Rotational speed	24	rad/s
p	Number of poles	2	1
P_{mind}	Minimum required power	0.67	kW
S	Number of slots or teeth on rotor	10	1
η	Motor efficiency	85%	1
ρ	Resistivity	1.68×10^{-8}	Ω·m
ρ_{Cu}	Density of copper	8900	kg/m^3
ρ_{Fe}	Density of iron	7900	kg/m^3
ψ	Pole arc to pole pitch ratio	0.66	1

Initial model before simplification

At this point, the motor subsystem optimal design problem is formulated below as:

$$\min\ W = \rho_{Cu}(A_{wa}L_{wa} + A_{wf}L_{wf}) + \rho_{Fe}L\pi(D + d_s)^2$$

Subject to:

$$h_1 = ac - \frac{2P_{\min_d}L_{wa}}{\pi\eta a n_d(2L + \frac{2.3\pi D}{p} + 5d_s)D}$$ Specific electrical loading

$$h_2 = I_f - \frac{A_{wf}^2 n_d}{h_f L_{mtf} b_{fc} f_{cf} p \rho}$$ Field current

$$h_3 = L_{mtf} - (L + 2b_{fc})$$ Mean turn length

$$h_4 = h_f - \frac{0.076\psi}{L}$$ Field winding height

$$g_1 = -L_{wa}$$ Positive length of armature wire

$$g_2 = -L_{wf}$$ Positive length of field wire

$$g_3 = -L$$ Positive rotor axial length

$$g_4 = -D$$ Positive rotor diameter

$$g_5 = -d_s$$ Positive depth of slots

$$g_6 = \frac{\pi D}{p} - 0.38$$ Pole pitch bound

$$g_7 = \frac{Lp}{\pi D} - 0.9$$ Length to pole pitch ratio upper bound

$$g_8 = 0.6 - \frac{Lp}{\pi D}$$ Length to pole pitch ratio lower bound

$$g_9 = \frac{2D}{D - 2d_s} - 3.5$$ Circumference to total teeth width ratio upper bound

$$g_{10} = 2.5 - \frac{2D}{D - 2d_s}$$ Circumference to total teeth width ratio lower bound

$$g_{11} = d_s - \frac{2\pi(D - 2d_s)}{s}$$ Slot depth bound

$$g_{12} = d_s - 0.5D$$ Slot depth bound

$$g_{13} = ac - 20$$ Specific electric loading upper bound

$$g_{14} = 6 - ac$$ Specific electric loading lower bound

$$g_{15} = \frac{1.2L_{wa}A_{wa}}{2L + \frac{2.3\pi D}{p} + 5d_s} - \pi[(\frac{D}{2})^2 - (\frac{D}{2} - d_s)^2]$$ Packaging-enough space for wrapped wires

$$g_{16} = 150 - \frac{(10l_f)^2 L_{wf}\rho}{A_{wf}(L_{mtf} + b_{fc})h_f}$$ Permissible heat loss per unit of surface area lower bound

$$g_{17} = \frac{(10l_f)^2 L_{wf}\rho}{A_{wf}(L_{mtf} + b_{fc})h_f} - 750$$ Permissible heat loss per unit of surface area upper bound

There are five design variables in total, which gives rise to a Degree of Freedom (DOF) of five. It should be noted here that although the initial formulation has four equality constraints (h_1-h_4), these constraints are only used to define the intermediate variables (*ac*, l_f, L_{mtf}, h_f) and thus do not affect the DOF. Another way to think about this is to consider the four intermediate variables as design variables with four equality constraints. Thus in this regard, the DOF is calculated as 9-4=5, which is the same result.

After substituting the values from table 2.3.2 for the design parameters, one feasible point can be found at:

$$\begin{aligned} L_{wa} &= 90 \\ L_{wf} &= 200 \\ L &= 0.1 \\ D &= 0.1 \\ d_s &= 0.01 \end{aligned}$$

It has been shown to be a feasible point by satisfying all the constraints of the model. This provides evidence that there is a feasible domain associated with the problem, so that further optimization procedures could be performed.

Next page summarizes the model in standard negative null form. The parameter values have been plugged into the model.

Summary model

After substituting the values from table 2.3.2, the design optimization problem for motor subsystem is summarized below in standard form:

$$\min\ W = 0.0178L_{wa} + 0.0089L_{wf} + 24818.58L(D + d_s)^2$$

Subject to:

$$\begin{aligned}
g_1 &= -L_{wa} \\
g_2 &= -L_{wf} \\
g_3 &= -L \\
g_4 &= -D \\
g_5 &= -d_s \\
g_6 &= D - 0.241916 \\
g_7 &= L - 1.413717D \\
g_8 &= 0.942478D - L \\
g_9 &= d_s - 0.2142857D \\
g_{10} &= -d_s + 0.1D \\
g_{11} &= d_s - 0.278431D \\
g_{12} &= d_s - 0.5D \\
g_{13} &= L_{wa} - 9565.446LD - 17279.17D^2 - 23913.62d_sD \\
g_{14} &= -L_{wa} + 2869.634LD + 5183.752D^2 + 7174.085d_sD \\
g_{15} &= L_{wa} - (2617994L + 4729185D + 6544985d_s)(Dd_s - d_s^2) \\
g_{16} &= 18.715L^3 + 5.895L^2 + 0.606L + 0.02 - L^3L_{wf} \\
g_{17} &= -93.574L^3 - 29.476L^2 - 3.032L - 1.029 + L^3L_{wf}
\end{aligned}$$

Variables: L_{wa}, L_{wf}, L, D, d_s

Number of equality constraints: 0

Number of inequality constraints: 17

Degree of freedom (DOF): 5

2.4 Model Analysis

This section conducts monotonicity analysis to simplify the problem. The monotonicity table for the original model (model 1) is provided in table 2.4.1 below.

Table 2.4.1: Monotonicity table for original model (model 1)

	L_{wa}	L_{wf}	L	D	d_s
W	+	+	+	+	+
g_1	-				
g_2		-			
g_3			-		
g_4				-	
g_5					-
g_6				+	
g_7			+	-	
g_8			-	+	
g_9				-	+
g_{10}				+	-
g_{11}				-	+
g_{12}				-	+
g_{13}	+		-	-	-
g_{14}	-		+	+	+
g_{15}	+			-	U
g_{16}		-	-		
g_{17}		+	+		

At a first glace of the monotonicity table, it could be noticed that g_9, g_{11} and g_{12} have the same monotonicity with respect to D and d_s, which is collected in the table below:

	L_{wa}	L_{wf}	L	D	d_s
W	+	+	+	+	+
g_9				-	+
g_{11}				-	+
g_{12}				-	+

Actually,

g_9 gives the relationship: $d_s \leq 0.2142857D$

g_{11} gives the relationship: $d_s \leq 0.278431D$

g_{12} gives the relationship: $d_s \leq 0.5D$

Therefore, g_{11} and g_{12} are dominated by g_9, and are redundant to the problem. After deleting the redundant constraints g_{11} and g_{12}, the reduced model (model 2) now looks like:

Model 2:

$$\min\ W = 0.0178L_{wa} + 0.0089L_{wf} + 24818.58L(D + d_s)^2$$

Subject to:

$$g_1 = -L_{wa}$$
$$g_2 = -L_{wf}$$
$$g_3 = -L$$
$$g_4 = -D$$
$$g_5 = -d_s$$
$$g_6 = D - 0.241916$$
$$g_7 = L - 1.413717D$$
$$g_8 = 0.942478D - L$$
$$g_9 = d_s - 0.2142857D$$
$$g_{10} = -d_s + 0.1D$$
$$g_{13} = L_{wa} - 9565.446LD - 17279.17D^2 - 23913.62d_sD$$
$$g_{14} = -L_{wa} + 2869.634LD + 5183.752D^2 + 7174.085d_sD$$
$$g_{15} = L_{wa} - (2617994L + 4729185D + 6544985d_s)(Dd_s - d_s^2)$$
$$g_{16} = 18.715L^3 + 5.895L^2 + 0.606L + 0.02 - L^3L_{wf}$$
$$g_{17} = -93.574L^3 - 29.476L^2 - 3.032L - 1.029 + L^3L_{wf}$$

The monotonicity table for model 2 is shown as:

Table 2.4.2: Monotonicity table for model 2

	L_{wa}	L_{wf}	L	D	d_s
W	+	+	+	+	+
g_1	-				
g_2		-			
g_3			-		
g_4				-	

g_5					-
g_6				+	
g_7			+	-	
g_8			-	+	
g_9				-	+
g_{10}				+	-
g_{13}	+		-	-	-
g_{14}	-		+	+	+
g_{15}	+			-	U
g_{16}		-	-		
g_{17}		+	+		

By monotonicity principle 1 (MP1) with respect to L_{wa}, at least one of g_1 and g_{14} must be active. Since $g_1 - g_{14} = -(2869.634LD + 5183.752D^2 + 7174.085d_sD) < 0$, it could be concluded that g_1 is dominated by g_{14} and it is redundant to the design problem. In addition, g_{14} is active. Therefore,

$$L_{wa} = 2869.634LD + 5183.752D^2 + 7174.085d_sD$$

The above equation is then substituted into the constraint g_{13}, which gives:

$$g_{13} = -6695.812LD - 12095.418D^2 - 16739.535d_sD \leq 0$$

This means that under the conclusion g_{14} is active, g_{13} is then satisfied. In other words, g_{13} is dominated by g_{14} and could be deleted from the problem. Now the design problem has the form shown on next page (model 3).

Model 3:

$$W = 51.0795LD + 92.2708D^2 + 127.6987d_sD + 0.0089L_{wf} + 24818.58L(D + d_s)^2$$

Subject to:

$g_2 = -L_{wf}$

$g_3 = -L$

$g_4 = -D$

$g_5 = -d_s$

$g_6 = D - 0.241916$

$g_7 = L - 1.413717D$

$g_8 = 0.942478D - L$

$g_9 = d_s - 0.2142857D$

$g_{10} = -d_s + 0.1D$

$g_{15} = (2869.634LD + 5183.752D^2 + 7174.085d_sD) - (2617994L + 4729185D + 6544985d_s)(Dd_s - d_s^2)$

$g_{16} = 18.715L^3 + 5.895L^2 + 0.606L + 0.02 - L^3L_{wf}$

$g_{17} = -93.574L^3 - 29.476L^2 - 3.032L - 1.029 + L^3L_{wf}$

Table 2.4.3: Monotonicity table for model 3

	L_{wf}	L	D	d_s
W	+	+	+	+
g_2	-			
g_3		-		
g_4			-	
g_5				-
g_6			+	
g_7		+	-	
g_8		-	+	
g_9			-	+
g_{10}			+	-
g_{15}			-	U
g_{16}	-	-		
g_{17}	+	+		

Similarly, by monotonicity principle 1 (MP1) with respect to L_{wf}, at least one of g_2 and g_{16} must be active. By comparing g_2 and g_{16}:

g_2 gives: $-L_{wf} \le 0$
g_{16} gives: $18.715 + 5.895L^{-1} + 0.606L^{-2} + 0.02L^{-3} - L_{wf} \le 0$

It follows directly that $g_2 - g_{16} = -18.715 - 5.895L^{-1} - 0.606L^{-2} - 0.02L^{-3} \le 0$, it could be concluded that g_2 is dominated by g_{16} and it is redundant to the design problem. In addition, g_{16} is active. Therefore,

$$L_{wf} = 18.715 + 5.895L^{-1} + 0.606L^{-2} + 0.02L^{-3}$$

The above equation is then substituted into the constraint g_{17}, which gives:

$$g_{17} = -74.859L^3 - 23.581L^2 - 2.426L - 1.009 \le 0$$

This means that under the conclusion g_{16} is active, g_{17} is then satisfied. In other words, g_{17} is dominated by g_{16} and could be deleted from the problem. The model is then further reduced to model 4:

Model 4:

$$W = 51.0795LD + 92.2708D^2 + 127.6987d_sD + (0.16656 + 0.0524655L^{-1} + 0.0053934L^{-2} + 0.000178L^{-3}) + 24818.58L(D + d_s)^2$$

Subject to:

$$g_3 = -L$$
$$g_4 = -D$$
$$g_5 = -d_s$$
$$g_6 = D - 0.241916$$
$$g_7 = L - 1.413717D$$
$$g_8 = 0.942478D - L$$
$$g_9 = d_s - 0.2142857D$$
$$g_{10} = -d_s + 0.1D$$
$$g_{15} = (2869.634LD + 5183.752D^2 + 7174.085d_sD) - (2617994L + 4729185D + 6544985d_s)(Dd_s - d_s^2)$$

Table 2.4.4: Monotonicity table for model 4:

	L	D	d_s
W	U	+	+
g_3	-		
g_4		-	
g_5			-
g_6		+	
g_7	+	-	
g_8	-	+	
g_9		-	+
g_{10}		+	-
g_{15}		-	U

Finally, the model could be further reduced by noticing that g_3 is dominated by g_8, and g_4 is dominated by g_7. Thus, g_3 and g_4 could also be deleted from the problem.

To conclude, the final reduced model is:

<u>Model 5:</u>

$$W = 51.0795LD + 92.2708D^2 + 127.6987d_sD + (0.16656 + 0.0524655L^{-1} + 0.0053934L^{-2} + 0.000178L^{-3}) + 24818.58L(D + d_s)^2$$

Subject to:

$$g_5 = -d_s$$
$$g_6 = D - 0.241916$$
$$g_7 = L - 1.413717D$$
$$g_8 = 0.942478D - L$$
$$g_9 = d_s - 0.2142857D$$
$$g_{10} = -d_s + 0.1D$$
$$g_{15} = (2869.634LD + 5183.752D^2 + 7174.085d_sD) - (2617994L + 4729185D + 6544985d_s)(Dd_s - d_s^2)$$

Table 2.4.5: Monotonicity table for model 5:

	L	D	d_s
W	U	+	+
g_5			-
g_6		+	
g_7	+	-	
g_8	-	+	
g_9		-	+
g_{10}		+	-
g_{15}		-	U

The reduced model now has 3 design variables (L, D, d_s) and 7 inequality constraints (g_5, g_6, g_7, g_8, g_9, g_{10}, g_{15}). The problem is well bounded based on the monotonicity principles.

To close the monotonicity analysis in this section, the work up to now could be summarized as follows:

Active constraints: g_{14}, g_{16}
Inactive constraints: g_1, g_2, g_3, g_4, g_{11}, g_{12}, g_{13}, g_{17}
Constraints with unknown activities: g_5, g_6, g_7, g_8, g_9, g_{10}, g_{15}
DOF after model reduction: 3

The determination of DOF could be addressed in two ways: The first way is to notice that original model has 5 DOF, and 2 active constraints are identified through the above monotonicity analysis. So now DOF will be 5-2=3. The second way is to look at the final reduced problem with 3 variables and no equality constraints, which also give 3 DOF.

It could be noted here that the expressions for the constraints do not have divisions of variables in order to avoid computational errors. The model now is ready to be implemented into the optimization package to obtain the numerical solutions.

2.5 Numerical Results

This section presents the numerical solutions to the motor subsystem design problem. The computation is done with the help of the MATLAB function 'fmincon'. The 'fmincon' function utilizes the Sequential Quadratic Programming (SQP) algorithm. It is useful in solving nonlinear, constraint, and continuous optimization problems (Optimal Design Laboratory, 2009). Therefore this method works well in this motor subsystem design optimization problem.

The optimization study is first performed on the original model without any reduction (5 variables and 17 constraints). The numerical solution is shown as:

$$W = 6.740353$$

$$\begin{aligned} L_{wa} &= 14.84918 \\ L_{wf} &= 452.9633 \\ L &= 0.0545918 \\ D &= 0.038616 \\ d_s &= 0.0038616 \end{aligned}$$

It should be noted that the units for all of the five design variables are in meters (m). The detailed MATLAB codes are provided in Appendix A.2.

The following sub-sections provide a detailed discussion on the optimization solutions, which includes: (1) Verification of monotonicity analysis, (2) Lagrange multipliers and constraint activities, (3) Global vs. local optima, (4) Satisfaction of KKT conditions

Verification of monotonicity analysis

To check the monotonicity analysis, the optimization study is then performed on the reduced model with 3 design variables and 7 inequality constraints (model 5). The optimal solution is found at:

$$W = 6.740349$$

$$L = 0.0545942$$
$$D = 0.038618$$
$$d_s = 0.0038618$$

Then, to determine the optimal solution for L_{wa} and L_{wf}, the above result is substituted into the active constraints identified in the monotonicity analysis:

$$L_{wa} = 2869.634LD + 5183.752D^2 + 7174.085d_sD$$
$$L_{wf} = 18.715 + 5.895L^{-1} + 0.606L^{-2} + 0.02L^{-3}$$

The result is:

$$L_{wa} = 14.85051$$
$$L_{wf} = 452.9236$$

The optimization results for both cases are collected in table 2.5.1 below.

Table 2.5.1: Numerical results comparison

Design	Original model	Reduced model	Percentage error
L_{wa}	14.84918	14.85051	0.009%
L_{wf}	452.9633	452.9236	-0.009%
L	0.0545918	0.0545942	0.0044%
D	0.038616	0.038618	0.00518%
d_s	0.0038616	0.0038618	0.00518%
W	6.740353	6.740349	-0.00006%

As indicated in table 2.5.1, the numerical results are consistent in both cases. The errors for the optimal solutions are all within 0.01% percent, which is acceptable. It is believed the two models actually generate the same optimal solution. The errors arise from the model reduction when there are some digits round-offs in the calculation. Therefore, this numerical result verifies the monotonicity analysis.

Lagrange multipliers and constraint activities

The 'fmincon' function is also capable of generating the Lagrange multipliers, which is summarized below:

Table 2.5.2: Lagrange multipliers

Constraints	Lagrange multipliers
g_1	5.38751006329041e-09
g_2	1.76614720886538e-10
g_3	1.46542213851771e-06
g_4	2.07169223403385e-06
g_5	2.07169275056664e-05
g_6	3.93506695817480e-07
$\boldsymbol{g_7}$	**97.2724824631822**
g_8	4.39626622843597e-06
g_9	1.81273056942024e-05
$\boldsymbol{g_{10}}$	**120.035519401807**
g_{11}	1.16106055840463e-05
g_{12}	5.17923028049169e-06
g_{13}	2.30893183211650e-09
$\boldsymbol{g_{14}}$	**0.0177999948896506**
g_{15}	2.48197041955306e-09
$\boldsymbol{g_{16}}$	**54.7026178279495**
g_{17}	6.53649981956433e-08

As highlighted in table 2.5.2, g_7 g_{10} g_{14} and g_{16} give a non-zero value of Lagrange multipliers. (The Lagrange multipliers for other constraints are less than the order of 10^{-5}

and are considered to be zero) It also indicates that these four constraints are active at optimality condition:

$$g_7 = L - 1.413717D = 0$$
$$g_{10} = -d_s + 0.1D = 0$$
$$g_{14} = -L_{wa} + 2869.634LD + 5183.752D^2 + 7174.085d_sD = 0$$
$$g_{16} = 18.715L^3 + 5.895L^2 + 0.606L + 0.02 - L^3L_{wf} = 0$$

This result could be easily verified by putting the numerical results obtained for the design variables:

$$L_{wa} = 14.84918$$
$$L_{wf} = 452.9633$$
$$L = 0.0545918$$
$$D = 0.038616$$
$$d_s = 0.0038616$$

This conclusion further verifies the monotonicity analysis. In monotonicity analysis, two active constraints are identified: g_{14} and g_{16}. With the help of computational approach, the other two active constraints (g_7 and g_{10}) are identified as well.

Another thing to notice here is that there are five variables but only four active constraints at optimality condition. The solution cannot be purely boundary solution because it still lacks one constraint to be active to give a system of five equations to solve for five variables. Therefore, the interior optima also come into play in order to solve this problem.

Global vs. local optima

The best way to tell if the results are global or local is to perform optimization study with different initial conditions. Here, four different initial conditions are selected arbitrarily to run the program. The results are shown on next page in table 2.5.3:

Table 2.5.3: **Optimal solutions with different initial conditions**

Design variables	L_{wa}	L_{wf}	L	D	d_s
Initial point 1	90	200	0.1	0.1	0.01
Optima 1	14.8491720	452.963292	0.05459178	0.03861578	0.00386158
Initial point 2	50	30	2	10	10
Optima 2	14.8521153	452.955103	0.05459256	0.03861662	0.00386199
Initial point 3	100	300	8	50	1
Optima 3	14.8491977	452.963287	0.05459178	0.03861578	0.00386158
Initial point 4	5	600	1	6	2
Optima 4	14.8497599	452.961649	0.05459194	0.03861594	0.00386166

It is obvious that the selection of initial conditions does not affect the location of optima. The initial conditions are arbitrarily chosen without any specific pattern. Although this result does not “prove” the global optimality, it does give evidence that the optimization results obtained from ‘fmincon’ function are most likely to be global minima other than local. It also shows that the problem is numerically stable.

Satisfaction of KKT conditions

To further interpret the numerical solutions, the Karush-Kuhn-Tucker (KKT) conditions are checked analytically to compare with the numerical results. It should be noted here that the existence of KKT points does not ensure the solution is a minimum since the conditions are not sufficient.

The KKT conditions for model in standard negative null form are:

$$\nabla f + \lambda^T \nabla h + \mu^T \nabla g = 0^T,$$
$$h = 0, g \leq 0,$$
$$\lambda \neq 0, \mu \geq 0, \mu^T \nabla g = 0.$$

To assist with the calculation, the model is rewritten in the form below. Here h_1-h_4 stands for the active inequality constraints in the original model (g_7, g_{10}, g_{14}, g_{16}). As proved previously, these four constraints are equal to 0 at optimality condition and could be treated as equality constraints.

$$\min\ W = 0.0178L_{wa} + 0.0089L_{wf} + 24818.58L(D + d_s)^2$$

Subject to:

$$h_1 = L - 1.413717D$$
$$h_2 = -d_s + 0.1D$$
$$h_3 = -L_{wa} + 2869.634LD + 5183.752D^2 + 7174.085d_sD$$
$$h_4 = 18.715L^3 + 5.895L^2 + 0.606L + 0.02 - L^3L_{wf}$$
$$g_1 = -L_{wa}$$
$$g_2 = -L_{wf}$$
$$g_3 = -L$$
$$g_4 = -D$$
$$g_5 = -d_s$$
$$g_6 = D - 0.241916$$
$$g_8 = 0.942478D - L$$
$$g_9 = d_s - 0.2142857D$$
$$g_{13} = L_{wa} - 9565.446LD - 17279.17D^2 - 23913.62d_sD$$
$$g_{15} = L_{wa} - (2617994L + 4729185D + 6544985d_s)(Dd_s - d_s^2)$$
$$g_{17} = -93.574L^3 - 29.476L^2 - 3.032L - 1.029 + L^3L_{wf}$$

The gradient of objective function:

$$\nabla W = \begin{pmatrix} 0.0178 \\ 0.0089 \\ 24818.58(D + d_s)^2 \\ (24818.58)(2)(L)(D + d_s) \\ (24818.58)(2)(L)(D + d_s) \end{pmatrix}^T = \begin{pmatrix} 0.0178 \\ 0.0089 \\ 44.78132 \\ 115.105 \\ 115.105 \end{pmatrix}^T$$

The gradient of equality constraint:

$$\nabla h = \begin{pmatrix} 0 & 0 & 1 & -1.413717 & 0 \\ 0 & 0 & 0 & 0.1 & -1 \\ -1 & 0 & 110.8138 & 584.7135 & 277.0345 \\ 0 & -0.00016 & -2.63289 & 0 & 0 \end{pmatrix}$$

The Lagrange multipliers are obtained from 'fmincon' function as:

$$\lambda = \begin{pmatrix} 97.27248246 \\ 120.0355194 \\ 0.017799995 \\ 54.70261783 \end{pmatrix}$$

To determine μ, it should be noted that all the inequality constraints are inactive according to the numerical results (g is not 0). Thus in order to satisfy: $\mu^T g=0$, μ has to be 0. Thus the KKT condition simplifies to:

$$\nabla W + \lambda^T \nabla h = 0^T,$$
$$h = 0, g \le 0,$$
$$\lambda \ne 0.$$

By putting the values into the above equation, the KKT condition is checked and satisfied. This means the results obtained from 'fmincon' are indeed KKT points.

$$\nabla W + \lambda^T \nabla h$$

$$= \begin{pmatrix} 0.0178 \\ 0.0089 \\ 44.78132 \\ 115.105 \\ 115.105 \end{pmatrix}^T + \begin{pmatrix} 97.27248246 \\ 120.0355194 \\ 0.017799995 \\ 54.70261783 \end{pmatrix}^T \begin{pmatrix} 0 & 0 & 1 & -1.413717 & 0 \\ 0 & 0 & 0 & 0.1 & -1 \\ -1 & 0 & 110.8138 & 584.7135 & 277.0345 \\ 0 & -0.00016 & -2.63289 & 0 & 0 \end{pmatrix}$$

$$= 0^T$$

2.6 Parametric Study

The optimal solutions discussed so far are obtained based on the parameter values listed in table 2.3.2. However, some of the parameter values are not well-known and might have uncertainties. These uncertainties would cause the optimal solution to change. Therefore, it is important to conduct parametric study to identify sensitivity of some parameters of interest.

In this section, four parameters are analyzed: cross-section of armature wire (A_{wa}), cross-section of field wire (A_{wf}), rotational speed (n_d) and minimum required power (P_{mind}). The reason to analyze these four parameters is: the wire cross-section areas are not right available and have to be estimated; the rotational speed and minimum required power are determined in the motor controller subsystem after running simulation although assumed constant in this subsystem. Each parameter is examined given ±10% perturbation of the original parameter value. The result is shown below in table 2.6.1.

Table 2.6.1: Parametric study

	L_{wa}	L_{wf}	L	D	d_s	W	Change in W
Original	15.12877	452.0359	0.055103	0.038977	0.003897	6.806448	
A_{wa} ↑	15.12876	452.0361	0.055103	0.038977	0.003897	6.833378	+0.395642%
A_{wa} ↓	15.12878	452.0358	0.055103	0.038977	0.003897	6.779519	-0.39564%
$\boldsymbol{A_{wf}}$ ↑	11.40918	450.1974	0.047852	0.033848	0.003384	6.256964	**-8.073%**
$\boldsymbol{A_{wf}}$ ↓	16.21710	579.6936	0.057050	0.040355	0.004035	7.722149	**+13.45343%**
$\boldsymbol{n_d}$ ↑	10.45332	449.6958	0.043672	0.030891	0.003089	5.439941	**-20.0767%**
$\boldsymbol{n_d}$ ↓	14.63161	520.4800	0.057121	0.040405	0.004040	7.693247	**+13.0288%**
P_{mind} ↑	13.75482	451.9912	0.055106	0.038979	0.003897	6.781977	-0.35954%
P_{mind} ↓	16.57564	458.2693	0.054718	0.038705	0.003870	6.835344	+0.424525%

As highlighted in table 2.6.1, the optimization result is most sensitive to the perturbation in field wire cross-section area (A_{wf}) and the rotational speed (n_d) during operation. On the other hand, the optimization result is less sensitive to the minimum require power

(P_{mind}) and the armature wire cross-section area (A_{wa}). This could be explained by the mathematical expression of field current and permissible heat loss per unit area:

$$I_f = \frac{A_{wf}^2 n_d}{h_f L_{mtf} b_{fc} f_{cf} p \rho}$$

$$pf = \frac{(10 I_f)^2 L_{wf} \rho}{A_{wf}(L_{mtf} + b_{fc}) h_f}$$

Both of A_{wf} and n_d appears in the field current expression, which is further squared to calculate the permissible heat loss per unit area. It makes sense these two parameters have the largest effect on the optimization results.

The parametric study also gives a warning on the careful determination of field wire cross-section area and the rotational speed of the motor. As implied by table 2.6.1, 10% perturbation of these parameter values will cause the optimal solution to change more than 8% (with even up to 20% change for rotational speed). Therefore, as a design engineer point of view, these two parameters have to be accurately determined with uncertainties not exceeding ±10% to make sure the optimization results be generalized.

It should be noted here that the rotational speed is to be determined from the motor controller subsystem in the simulation analysis. Therefore, this parametric study is to be used as a reminder on the later system integration process.

Another thing of interest here is to see if changing parameter values will affect the constraint activity. Table 2.6.2 on next page lists the Lagrange multipliers in all cases. As highlighted in the table, the Lagrange multipliers for g_7, g_{10}, g_{14} and g_{16} are non-zero in all cases. This implies these four constraints remain active despite perturbation in the design parameters of interest.

Table 2.6.2: Lagrange multipliers

Constraints	A_{wa} ↑	A_{wa} ↓	A_{wf} ↑	A_{wf} ↓	n_d ↑	n_d ↓	P_{mind} ↑	P_{mind} ↓
g_1	0	0	0	0	0	0	0	0
g_2	0	0	0	0	0	0	0	0
g_3	0	0	0	0	0	0	0	0
g_4	0	0	0	0	0	0	0	0
g_5	0	0	0	0	0	0	0	0
g_6	0	0	0	0	0	0	0	0
$\boldsymbol{g_7}$	**49.90082**	**49.12434**	**37.85462**	**52.93521**	**32.13180**	**47.39053**	**37.47756**	**38.15447**
g_8	0	0	0	0	0	0	0	0
g_9	0	0	0	0	0	0	0	0
$\boldsymbol{g_{10}}$	**24.54836**	**24.34975**	**18.57072**	**26.17225**	**15.62138**	**23.47461**	**18.46828**	**18.63912**
g_{11}	0	0	0	0	0	0	0	0
g_{12}	0	0	0	0	0	0	0	0
g_{13}	0	0	0	0	0	0	0	0
$\boldsymbol{g_{14}}$	**0.049328**	**0.040370**	**0.034507**	**0.048110**	**0.031742**	**0.038914**	**0.030938**	**0.037802**
g_{15}	0	0	0	0	0	0	0	0
$\boldsymbol{g_{16}}$	**160645.2**	**158523.0**	**82819.89**	**203697.6**	**58096.09**	**133762.4**	**82055.19**	**83287.58**
g_{17}	0	0	0	0	0	0	0	0

2.7 Discussion of Results

The optimization so far is based on the mathematical model for the motor subsystem. Now it is a good time to translate the mathematical interpretation of the problem back into its engineering meaning.

First of all, the results obtained can be summarized as:

Length of armature wire: 14.85 meters
Length of field wire: 452 meters
Rotor axial length: 0.0546 meters (5.46 cm)
Rotor diameter: 0.03862 meters (3.862 cm)
Depth of slots: 0.003862 meters (3.862 mm)

And the minimum weight for the designed motor is 6.74 kg.

The result is reasonable based on the design guidelines in (Hamdi, 1994). The armature length should be in a certain range to meet the specific electric loading requirements. The field wire should be long enough in order to carry the field current and at the same time provide an allowable range of permissible heat loss. The depth of slots should be around 1/10 of the rotor diameter to provide enough packaging space for the wrapped wires.

The minimum weight is 6.74 kg and is applicable in the electric-bicycle application. This weight is lower than the one of 14 kg determined in previous research (Julie, 2002). The reason is that since this motor will be applied to the electric-bicycle system, it has to be smaller in size and lighter in weight than normal DC motor to fit more easily into the bicycle structure.

Another factor not appearing in this optimization study is the tooth flux density constraints. Careful design in this case would avoid the problem of "high-frequency iron loss" (Hamdi, 1994), which is common in DC machines. This is not addressed in this study due to the lack of information on flux density formulation. Future work is recommended to take this factor into account to improve the current motor design.

Finally, the optimization results so far are based on the motor subsystem alone. However, when integrated together into the overall electric-bicycle system, more factors need to be considered such as the armature resistance and motor moment of inertia. These two quantities are actually functions of the design variables in this subsystem, and will be used in the motor controller subsystem to obtain the dynamic behavior of the entire system.

Next part (starting from next page) details the work done to obtain the optimal solutions for motor controller subsystem in order to achieve control accuracy by choosing the optimal control gains.

DC-Motor Controller Subsystem Design – Rongtao Jia

2.1 Problem Statement

DC motor generates motion with power which is offered from battery. Between them, a controller is necessary to control circuitry in the form of analog or digital input signals. In this project, a proportional–integral–derivative controller (PID controller) controller is designed to adjust the speed of motor with high accuracy, small effort and short response time. A PID controller is a generic control loop feedback mechanism (controller) widely used in industrial control systems – a PID is the most commonly used feedback controller. Users can modify the dynamic properties of this controller by adjusting the three parameters. A PID controller calculates an "error" value as the difference between a measured process variable and a desired set point. An expected speed will be set and the controller adjusts the power from battery to motor to achieve the set speed. However, the PID controller has inherent tradeoffs between output power and controllability – meaning accuracy and response. As motor power output increases, the transient response and overshoot are negatively affected. In addition, practical designs of controller are affected by rotor inertia and motor constraints as well as dimension constraints.

DC motor design and controller design are two interactional subsystems. The parameters of plant (motor) affect the choice of PID controller and these parameters are also the design variables in motor subsystem. There currently is no practical means which can be used to design a controller/DC motor system to optimize all the objectives. The best available method is to use the interaction between the two subsystems to try solutions to get the most available optimization result for the two objective functions.

The controller part attempts to develop an optimization model and its objective is to optimize the output speed response performance, which can be expressed by minimize the integral of errors between the reference and the output speed. Meanwhile the model should meet controller’s defined constraints on response properties used to formulate a “best” one for the whole system.

2.2 Nomenclature

Symbols	Description
B	Rolling resistance
EMF	Electro-Magnetic Force
R_a	Armature resistance
I_a	Armature current
V_a	Voltage offered by battery
V_c	Voltage offered after controller processing
M_p	Maximum overshoot
t_s	Settling time
ξ	Motor damping ratio
J	Inertia
k_v	Back-EMF constant
k_t	Torque constant
L_a	Armature inductance
ω	Rotational speed
T_{load}	Load torque
T_e	Electric torque
T_{net}	Net torque
Ψ	Pole arc to pole pitch ratio
T	Time
Kp	Proportional value in PID controller
Ki	Integral value in PID controller
Kd	Derivative value in PID controller

2.3 Mathematical Model

Objective function

The objective is to minimize the integral of errors between the reference and the output speed within controller's defined constraints on response properties used to formulate a "best" one for the whole system. To generate the objective function, a simple analysis of the control system is necessary.

For a DC motor, the electrical equivalent circuit has the three equations:

$$V_c = R_a I_a + L_a \frac{dI_a}{dt} + k_v \omega \quad (1)$$

$$EMF = k_v \omega \quad (2)$$

$$T_e = k_t I_a \quad (3)$$

The back-EMF voltage is given by the product of back-EMF constant k_v and rotor speed ω. The mechanical equivalent circuit has the following equation (A. Muetze, 2007):

$$T_{net} = T_e - T_{load} = J\frac{d\omega}{dt} + B\omega$$

T_{load} is known parameter at any time and can be obtained from its profile. The torque output from motor is T_e.

For an excellent performance of control response, its errors between reference and output speed are relatively small, which means the control is accurate and steady. To compare the performance between different designs, we can calculate the integral of the time multiplied by the absolute error value during the time [0, t]. This is an index to evaluate the performance. So the objective function is to minimize:

$$F = f(k_i, k_p, k_d) = \int_0^t abs(Reference - output\ speed)$$

Where k_i, k_p, k_d are the design variables in PID controller. The physical meaning of them is to direct to build the PID controller circuit with resistance,

The corresponding block diagrams are shown in Fig. 1 and Fig. 2.

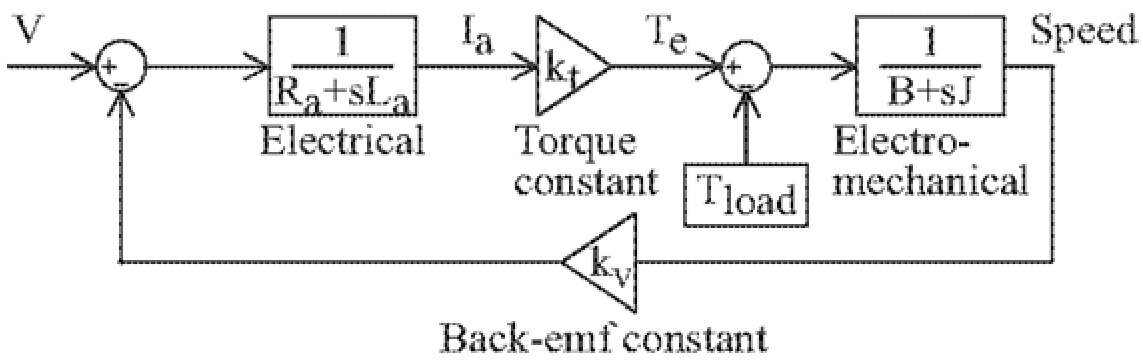

Fig. 1: Motor model block including mechanical equation

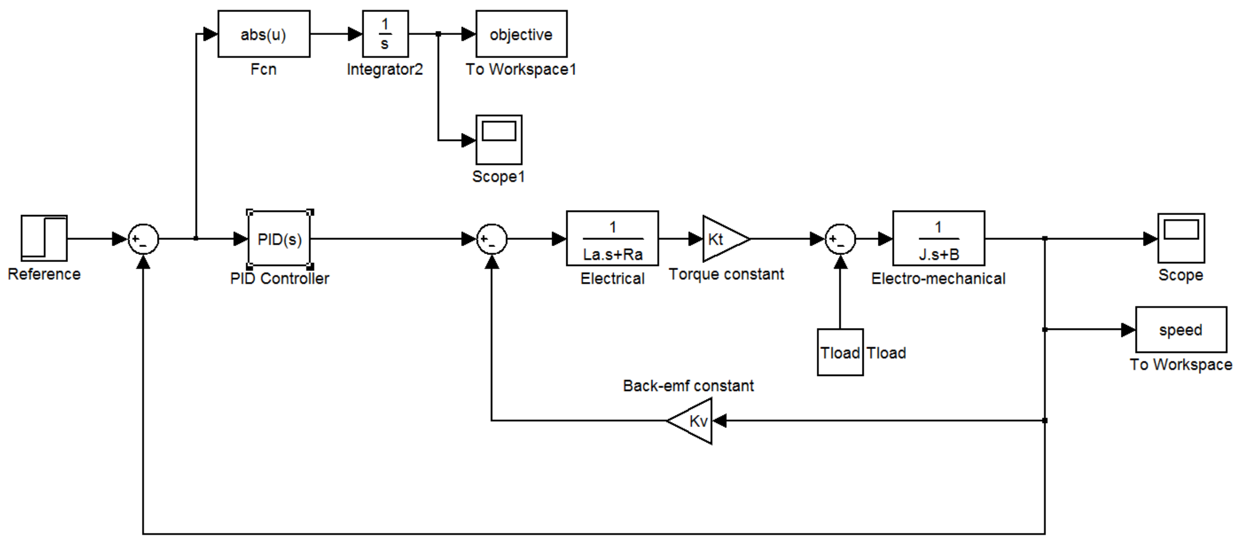

Fig. 2: Motor model and PID Controller block in Simulink

Reference in Fig. 2 means the desired speed set by users. The output speed is acquired in the end of the loop and recorded in the workspace of speed. The workspace records all the values during the whole running time. The integrals of the difference between reference and output speed are logged in workspace of objective. The last value of objective workspace is the value of objective function after a running time t.

Constraints

Subject to	g_1: $\omega \le 30$ rad/s	Motor rotational speed
	g_2: $0 \le \omega$	Motor rotational speed
	g_3: $T_e \le 80$ N*m	Torque generated in motor
	g_4: 5 N*m $\le T_e$	Torque generated in motor
	g_5: $\xi \le 1$	Motor damping ratio
	g_6: $0 \le \xi$	Motor damping ratio
	g_7: $M_p \le 35\%$	Max overshoot of speed response
	g_8: $0 \le M_p$	Max overshoot of speed response
	g_9: $t_s \le 5$s	Settling time of speed response
	g_{10}: $0 \le t_s$	Settling time of speed response
	g_{11}: $V_a \le 50$V	Voltage input
	g_{12}: 10V $\le V_a$	Voltage input

The constants in these constraints are determined by the average values in the other subsystems and regular values for a similar electric bicycle with a DC motor. Because of the interaction between subsystems, they may be changed with the system optimization like V_a. In this stage, they are determined to run optimization in controller subsystem.

Based on second Monotonicity Principle, some constraints are added to give a well-boundedness for the variables which do not appear in objective function and relevant. g_1, g_2, g_3 and g_4 mean that the angular speed of the motor and torque produced have the constraints from above and below. They determine the range of reference speed with g_7. g_5 and g_6 shows the motor damping coefficient should be between 0 and 1. This ensures that the system cannot be overdamped which always has a long settling time. g_7 and g_8 gives M_p an upper limit to give a low distortion and an theoretical lower limit. g_9 gives a longest settling time which can be accepted. g_{11} and g_{12} give the range of V_a from battery subsystem.

All of the constraints are practical constraints. g_1, g_2, g_3 and g_4 are determined by the current engineering practice. They would not be there without consideration of technique. g_5 to g_{10} are determined by the practical experience. In PID control problem, there is no quantitative functions to express damping ratio, maximum overshoot and settling time with k_p, k_i, and k_d. g_{11} and g_{12} are acquired from the parameters of the battery for bicycle use which is limited by the current techniques. By now, we cannot determine the activities of the constraints. These will be analyzed in the following parts which include the modal analysis with fmincont function in Matlab.

Design variables and parameters

Design variables

- k_p proportional gain
- k_i integral gain
- k_d derivative gain

Parameters

• B	Rolling resistance	0.01 N*s/m
• L_a	Armature inductance	0.5 H
• J	Inertia	0.5 kg*m^2
• R_a	Armature resistance	0.1 Ω
• k_t	Torque constant	5 N*m/A
• k_v	Back-EMF constant	0.5 V*s/rad
• T_{load}	Load torque	1 N*m
• V_a	Voltage offered by battery	depend on battery system
• T	Time	30s

There are only three design variables in this subsystem. B, R_a, L_a, V_a, J, T_{load}, k_t and k_v are assumed as constants and they can be expressed with the variables in the motor and battery subsystem. V_c and I_a are determined by the three variables of PID controller. T is the time of simulation. That means the variables in motor subsystem affect the parameters in controller design. There are no equalities in the constraints. The three design variables are independent with each other. The system has three degrees of freedom.

Validate the feasibility of optimization model

Example

Minimize $F = f(k_i, k_p, k_d) = \int_0^t abs(Reference - output\ speed)$

Subject to	g_1: $\omega \le 30$ rad/s	Motor rotational speed
	g_2: $0 \le \omega$	Motor rotational speed
	g_3: $T_e \le 80$ N*m	Torque generated in motor
	g_4: 5 N*m $\le T_e$	Torque generated in motor
	g_5: $\xi \le 1$	Motor damping coefficient
	g_6: $0 \le \xi$	Motor damping coefficient
	g_7: $M_p \le 35\%$	Maximum overshoot of speed response
	g_8: $0 \le M_p$	Maximum overshoot of speed response
	g_9: $t_s \le 5$s	Settling time of speed response
	g_{10}: $0 \le t_s$	Settling time of speed response
	g_{11}: $V_a \le 50$V	Voltage input
	g_{12}: 10V $\le V_a$	Voltage input

The parameters used in the test are:

B = 0.01N*s/m R_a = 0.1 Ω

L_a = 0.5H J = 0.05kg*m^2

k_v = 0.5 k_t = 5

T_{load} = 1 N*m T = 10s

After setup Simulink model and run, the response of speed is shown in Fig. 3. The torque generated in motor is shown in Fig. 4.

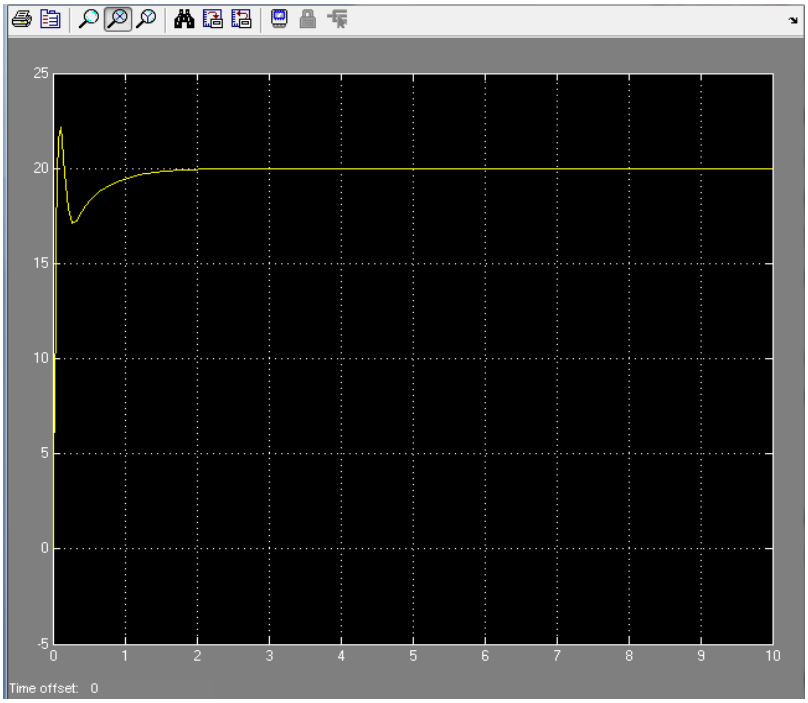

Fig. 3: Speed response of motor with PID controller

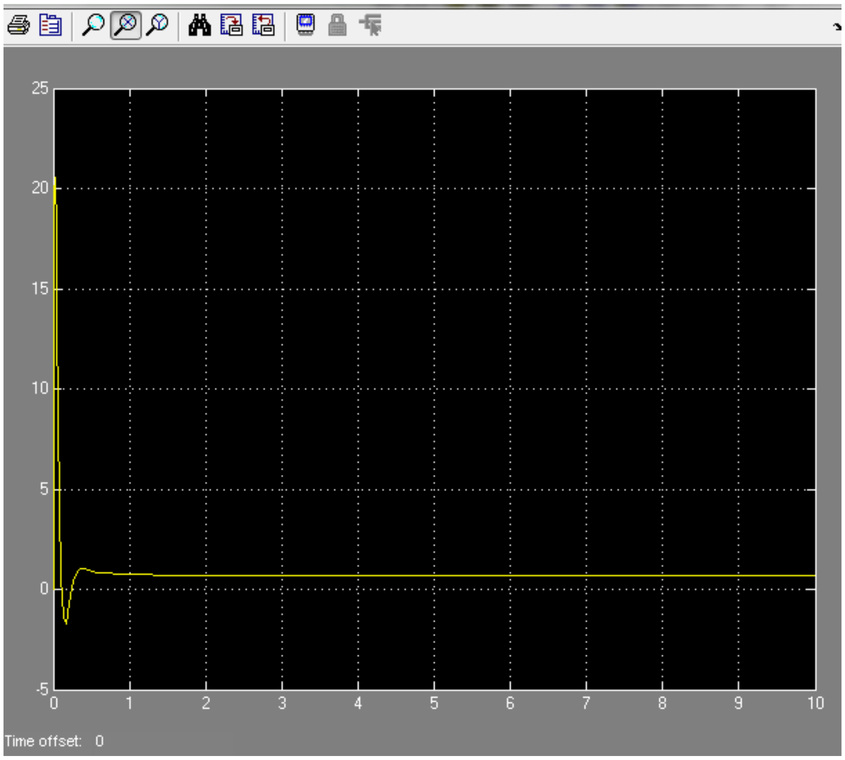

Fig. 4: Torque generated in motor

From Fig. 3, ξ = 0.65, maximum overshoot = 10%, settling time = 1.8s. From Fig. 4, maximum Torque generated in motor is 21 N*m. The solution of k_p = 1.24, k_i = 3, and k_d = 0.1 is feasible. This confirms the optimization model is complete and feasible.

Summary model

The objective is to minimize the integral of errors between the reference and the output speed.

Minimize	$F = f(k_i, k_p, k_d) = \int_0^t abs(Reference - output\ speed)$	
Subject to	g_1: $\omega \leq 30$ rad/s	Motor rotational speed
	g_2: $0 \leq \omega$	Motor rotational speed
	g_3: $T_e \leq 80$ N*m	Torque generated in motor
	g_4: 5 N*m $\leq T_e$	Torque generated in motor
	g_5: $\xi \leq 1$	Motor damping ratio
	g_6: $0 \leq \xi$	Motor damping ratio
	g_7: $M_p \leq 35\%$	Max overshoot of speed response
	g_8: $0 \leq M_p$	Max overshoot of speed response
	g_9: $t_s \leq 5$s	Settling time of speed response
	g_{10}: $0 \leq t_s$	Settling time of speed response
	g_{11}: $V_a \leq 50$V	Voltage input
	g_{12}: 10V $\leq V_a$	Voltage input

As motioned, the constants in these constraints are determined by the average values in the other subsystems and regular values for a similar electric bicycle with a DC motor. These values will be modified with the optimization solutions in the other subsystems and making a final decision.

2.4 Model Analysis

Monotonicity analysis

It is useful to observe the influence of individual design variables on the objective function. This helps identify potential issues with the optimization model and key variables to scrutinize.

	k_p	k_i	k_d
F	U	U	U
G1	implicit	implicit	implicit
G2	implicit	implicit	implicit
G3	implicit	implicit	implicit
G4	implicit	implicit	implicit
G5	-	-	+
G6	+	+	-
G7	+	+	_
G8	-	-	+
G9	U	+	-
G10	U	-	+
G11	U	U	U
G12	U	U	U

Table 1: Monotonicity analysis of the model

g_1 and g_2 are constraints of motor speed, which is a setup reference to controller. So, it is independent with the three design variables. These two constraints seem to be redundant, but they are still important in the design model. The maximum overshoot percentage is relative to the motor speed. The maximum overshoot speed value should be in the range of the constraints. g_{11} and g_{12} have the similar situation. The voltage on the motor is processed after controller not the one from the battery directly. But the voltage going into controller is constrained by g_{11} and g_{12}. The monotonicity analysis of

g_5 to g_{10} is based on Table 2. There are not exact control relationship between the variables and property parameters.

Parameter	Rise time	Overshoot	Settling time	Steady-state error	Stability
k_p	Decrease	Increase	Small change	Decrease	Degrade
k_i	Decrease	Increase	Increase	Decrease significantly	Degrade
k_d	Minor Decrease	Minor Decrease	Minor decrease	No effect in theory	Improve if k_d small

Table 2: Effects of increasing a parameter independently

In a second order system, the damping ratio determines the overshoot. The plot of % overshoot vs Damping ratio is shown in Fig. 5. Then the monotonicity analysis of g_5 and g_6 can be done.

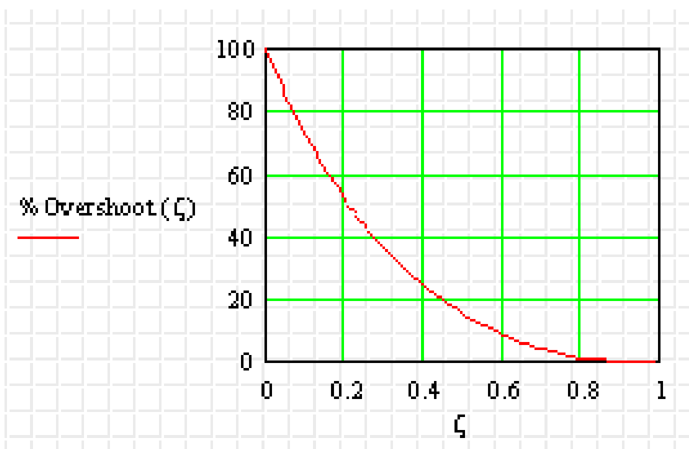

Fig. 5: The plot % overshoot vs damping ratio

From Table 1, the three design variables all have above and below constraints. The constraints which bound the variables are monotonic. In the case of the simulation, it is not obvious where monotonicities exist. This is the hardest part of this model. The main program uses fmincon to find optimal solution. The objective function will call the model in Simulink to get the objective value for different design variables. The constraint function will also call the model to do simulation to check if the design solution meets the constraints. There is no numerical function but a black box. An appropriate initial guess is important.

Model reduction

g_1, g_2, g_3, g_4, g_{11}, and g_{12} do not have many effects on the optimization of controller design. They are independent with the design variables in controller systems. They are more like constraints of parameters. With these, they can be eliminated from the model. The optimization solution will give the output speed a steady state, which means the damping ratio ξ will meet the constraints of g_5 and g_6. These two constraints can be deleted too. So, the new reduced model just has four constraints of the response properties: maximum overshoot and settling time. The new model in negative null form is shown below:

Minimize	$F = f(k_i, k_p, k_d) = \int_0^t abs(Reference - output\ speed)$	
Subject to	g_1: $M_p - 35\% \le 0$	Max overshoot of speed response
	g_2: $-M_p \le 0$	Max overshoot of speed response
	g_3: $t_s - 5s \le 0$	Settling time of speed response
	g_4: $-t_s \le 0$	Settling time of speed response

Constraint activity identification

For PID controller system, it is hard to use activity matrices to identify active or conditionally active constraints because of the implicit relationship of the design variables and parameters. These can be done by fmincon. It will give the Lagrange multipliers at solution, which can help to identify the activities of constraints.

Simulink black box

The whole loop is shown in Fig. 2. Because of the existence of PID controller, the transfer function of output speed is not second order. As known, a second order system can use numerical functions to express maximum overshoot and settling time. For a higher order system with symbolic parameters, it is hard to express them with an explicit relationship. In the model, we use workspace to collect data for objective function values and output speed. Based on these, we can get the objective function and constraint function values after running time t. Simulink model acts as a black box with implicit functions here. The inputs are the three design variables. The output is the optimal solution and objective function value.

Matlab optimization tool

Constraints

maximum overshoot

From the definition of maximum overshoot shown below, we can get the maximum value from the output speed workspace easily to derive the value of maximum overshoot of the speed's response. The Matlab codes are shown in Appendix A.3

$$Maximum\ overshoot = 100 * \frac{\text{Max value} - \text{Reference}}{\text{Reference}} \%$$

settling time

The settling time is the time elapsed from the application of an ideal instantaneous step input to the time at which the amplifier output has entered and remained within a specified error band, usually symmetrical about the final value. Settling time includes a very brief propagation delay, plus the time required for the output to slew to the vicinity of the final value, recover from the overload condition associated with slew, and finally settle to within the specified error. In this project, the error band is set as 3%. We search for the first point outside the error band and return its time in the direction from the final time t= 30s to initial time t=0s. The Matlab codes are shown in Appendix A.3

Objective function

The objective function values can be acquired directly from the objective workspace. It just needs to run the simulation and read the last value of the workspace. The Matlab codes are shown in Appendix A.3

Mainprograms

This part defines the global variables and parameters used in the whole model. We use fmincon to run the optimization process. In fmincon, it calls FUN.m and NONLCON.m to get the objective function and constraint function values. After running, we can get the optimal solution. The algorithm used in fmincon is Sequential quadratic programming (SQP). The Matlab codes are shown in Appendix mainsteps.m.

The parameters used in this system are fixed. They can be changed based on the optimal solutions from other subsystems.

2.5 Optimization Study

Solution identification

The initial guess used in the optimization process are Kp = 0.813, Ki = 1.435, and Kd = 0.1111. These guesses are based on a normal tuning range of PID controller. The initial values are typed in manisteps.m. Then run the program and we will get the results including the optimal solution, objective value, a structure lambda whose fields contain the Lagrange multipliers, the value of the gradient of objective function and the values of the Hessian at the solution x. The results are shown below:

```
xopt =

    0.8232    1.4551    0.1111


fval =

   12.9376

output =

         iterations: 2
          funcCount: 133
          algorithm: 'sequential quadratic programming'
            message: [1x702 char]
    constrviolation: 19.7985
           stepsize: 3.1197e-007
       firstorderopt: 19.7985

grad =

         0
   -1.1627
    8.1263
```

hessian =

1.0e+012 *

3.2409	2.2274	3.2409
2.2274	1.5309	2.2274
3.2409	2.2274	3.2409

g_1 = -11.16;
g_2 = - 23.84%;
g_3 = -0.37s
g_4 = -4.63s

The response and objective plots are shown in Fig. 6 and Fig. 7.

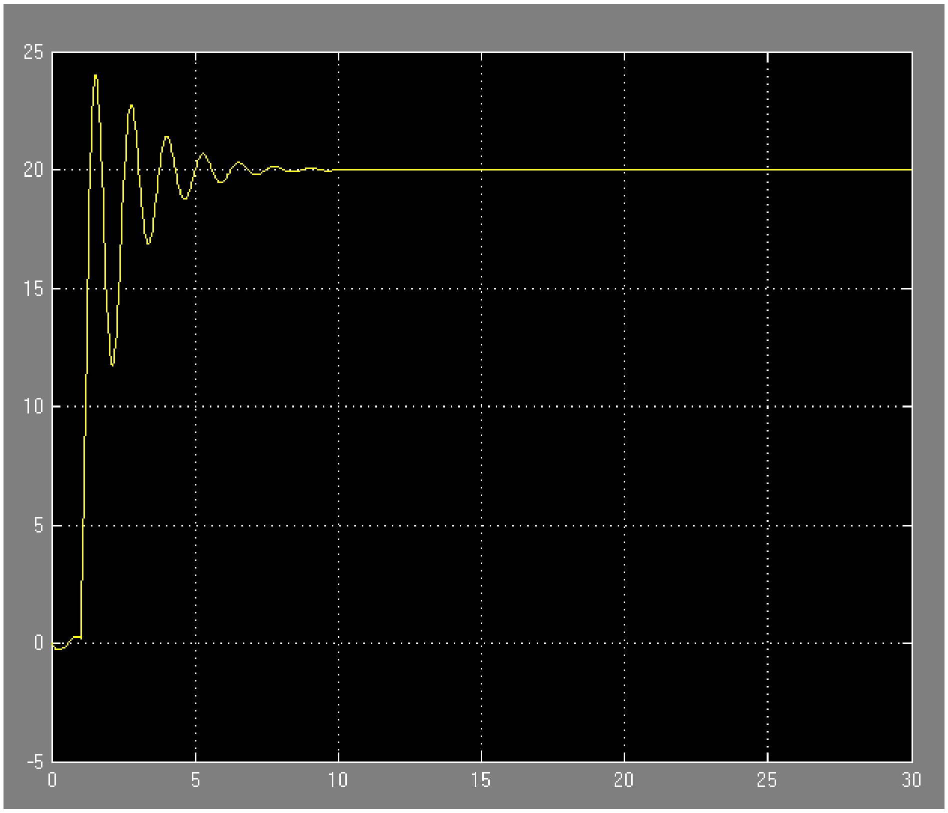

Fig. 6 The response of output speed

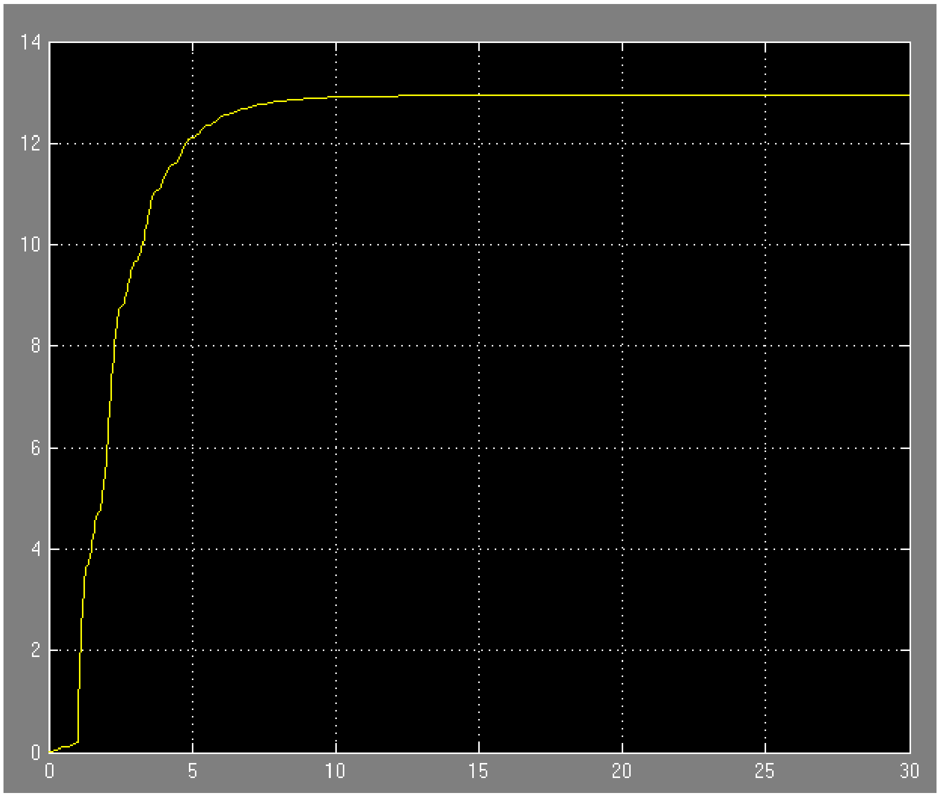

Fig. 7 The objective value increases to a steady state.

The optimal solution is Kp = 0.8232, Ki = 1.4551, Kd = 0.1111. The objective function value is 12.9376. From the values of gradient at solution, the solution is not a stationary point. This is not a simple solution to be evaluated by a local or global optimal solution. This will be discussed later.

Constraint activity analysis with Lagrange multipliers

Though there is no equality constraints in the subsystem, fmincon treats the inequality constraints as equality ones to get the Lagrange multipliers to check their activities. From the results of the optimization, we get the Lagrange multipliers of the constraints shown in Table 3.

Constraint	G1	G2	G3	G4
Multipliers	8.3573*E(-8)	7.4982*E(-10)	2.3905*E(-7)	5.9327*E(-8)

Table 3: The Lagrange multipliers for the four constraints

The multipliers are very close to 0 and can be treated as 0. These show that none of them is active. This is impenetrable for an optimal problem. The reason for this is mostly from the nature of the PID controller. For the implicit objective function, it is hard to apply KKT conditions to check it s satisfaction. The black box is complicated.

Analysis of optimal solution

The above results offer little help to determine the properties of the optimal solution. It is hard to check if it is global or local optimum. The optimal solution should be an interior solution, because the three design variables are all in an open domain.

We tried different initial guesses and got different solutions. Combined with the complicated nature of PID controller, it makes some sense. Different from the other design systems, PID controller system is not stable when we change the three design variables. That means the system is dependent with them. A new set of the variables creates a new system. It causes problems for fmincon to find optimal solution with a changing system when it tests different values for the variables.

The simulation model in Simulink is completed. The best solution to get a better solution for this subsystem is to collect large amount of feasible data to compare in a visual graph. It will take a lot of time. The strategy is to set several initial guesses and run the model to get enough data in its feasible domain.

The following is part of the current stage. Here takes one initial guess as an example to show the procedure. The table below shoes the data collection for different starting points.

k_p	k_i	k_d	Objective value
0.8332	1.4551	0.1211	12.9371
0.8128	1.4452	0.1211	11.4835
0.8232	1.3451	0.1311	13.2872
0.7231	1.2451	0.1311	12.6453
0.7431	1.4451	0.1411	14.3822
0.6532	1.3451	0.1511	13.2175
0.9932	1.3451	0.1511	11.6746
0.9932	1.4451	0.1432	12.9374
0.9832	1.4451	0.1255	13.1147
0.9732	1.2432	0.1288	12.5374
0.9522	1.1432	0.1322	13.0473
0.9322	1.1432	0.1222	12.4852
0.9322	1.1322	0.1511	11.8754

Table 4: Data collection of different initial guesses

We should noticed that there is a high possibility to get a local optima instead of global one based on this method of initial guesses. A good way to avoid this defect is to make more initial guesses with a relative long distance between each other. We are trying to make the method more efficiently with interaction with the other subsystems. The model needs to do more simulation based on the other subsystems' optimal solutions. The uncertainty of PID controller system is the main reason for taking much time to find optimal solution.

2.6 Parametric Study

The above optimal solution is obtained based on the parameter values listed in 2.3 Mathematical Model. However, some of the parameter values are not fixed and might change a lot from the optimization of other subsystems. These would give different sets of parameters values, which may cause a different optimal solution. Therefore, parametric study is necessary to identify sensitivity of the parameter values.

In this section, five parameters are analyzed: rolling resistance (B), inertia (J), armature resistance (R_a), armature inductance (L_a) and reference speed (W_0). Each parameter is examined given ±10% perturbation of the original parameter value. The result is shown below in Table 5.

	B	J	R_a	L_a	W_0	*Objective*	Change in W
Original	0.01	0.5	0.1	0.5	20	12.9376	
B ↑	0.0101	0.5	0.1	0.5	20	13.1274	+1.4670%
B ↓	0.0099	0.5	0.1	0.5	20	12.7563	-1.4013%
J ↑	0.01	0.505	0.1	0.5	20	11.9734	-7.4527%
J ↓	0.01	0.495	0.1	0.5	20	12. 7438	-1.4980%
R_a ↑	0.01	0.5	0.101	0.5	20	14.5063	+12.1251%
R_a ↓	0.01	0.5	0.099	0.5	20	12.0472	-6.8823%
L_a ↑	0.01	0.5	0.1	0.505	20	13.2436	+2.3652%
L_a ↓	0.01	0.5	0.1	0.495	20	12.0013	+7.2370%
W_0 ↑	0.01	0.5	0.1	0.5	20.2	10.1208	-21.77%

W_0 ↓	0.01	0.5	0.1	0.5	19.8	14.1868	+9.6556%

Table 5: Parametric study

From Table 5, the optimization result is most sensitive to the reference speed and armature resistance. Meanwhile, the optimization solution is less sensitive to the rolling resistance and the armature wire cross-section area. The results suggest that the controller has a better performance when the reference speed is higher.

There seems no clear relationship between the changes of parameters and system performance. This study still gives us some ideas about the design of the system. This table is acquired just using 10 percents of perturbation. The optimum changes with similar percentages. In the system integration part, these parameters may diverse with a larger percents, and the modal may have some problems like unstable simulation. The table is valuable to give some constraints to other subsystems to determine the range of their design variables.

Therefore, the parametric study is to be used as a reminder on the later system integration process.

2.7 Discussion of Results

The controller system design gives the optimal solution including the values for Kp, Ki, and Kd. These values help us to build the real circuit with the principles show in Fig. 8. The real circuits will act as an approximate ideal PID controller based on the theoretical electric functions.

This subsystem is an implicit black box optimization problem and it is affected by every little change of parameters and design variables. This property of PID controller causes a lot of problems on using the methods learned in class to solve. With the help of Matlab and optimization toolkit, we still get some useful results and optimal solution.

In the study process, I have found some design rules for this subsystem. Firstly, the initial guesses are very important. As described early, the initial guess will make the system different because they are not independent. After having an appropriate initial guess to meet the constraints, we need to be careful to try different starting points based on the first one. A random guess may cause the system unstable. We should change the starting point a little by little while make sure they are feasible for the system. Second point is the stability of system is most important. An unstable system caused by unfeasible solutions will use a lot of time and memory of computer to get a useless and wrong solution. Therefore, it is really a heavy task to get feasible and various initial guesses to run the program to get optimal solutions.

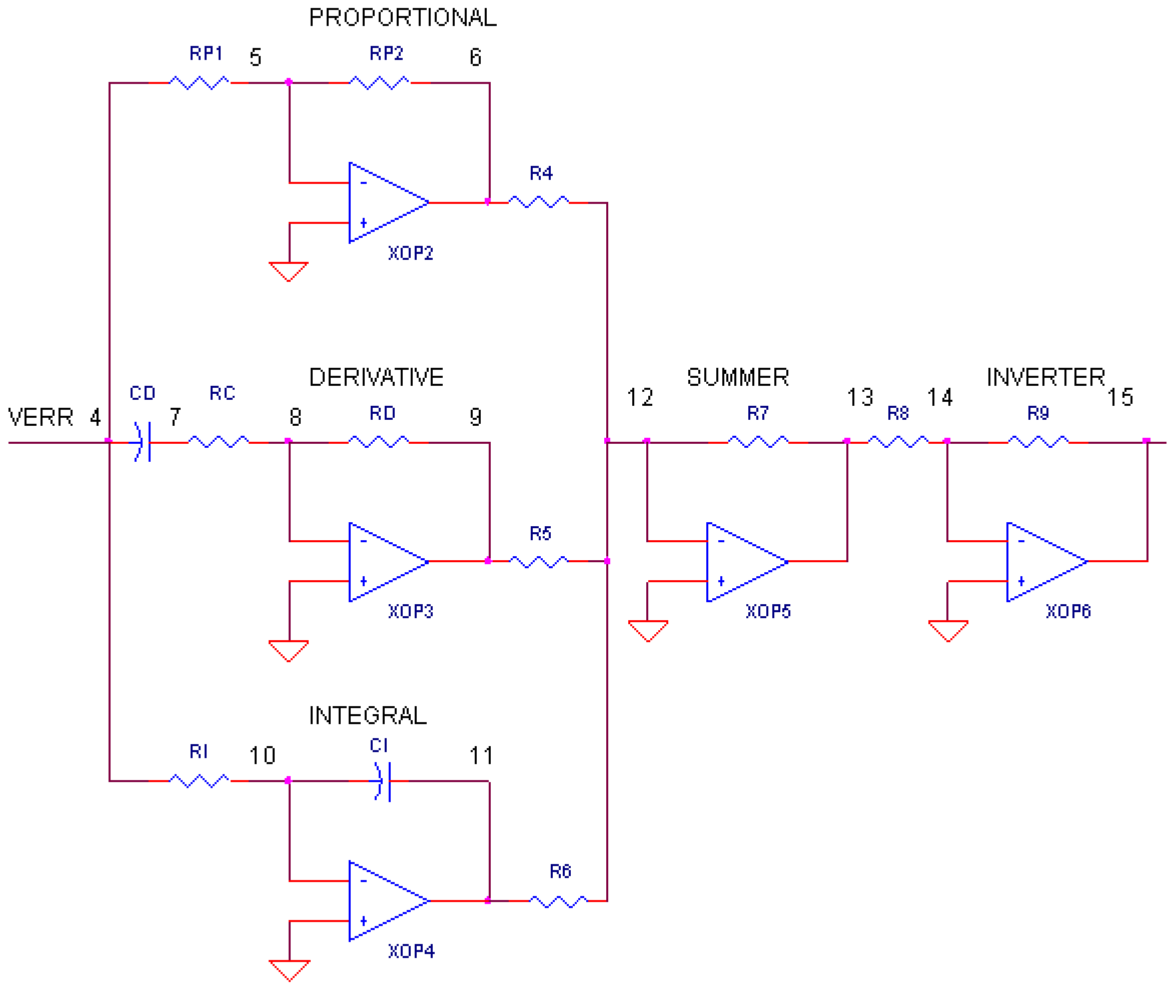

Fig. 8: The circuit of an OP Amp PID controller

Because the stability has a high requirement for the parameters, this subsystem can treated as some constraints for the rest subsystems. The optimal solutions for the rest systems need to ensure the stability of controller. The design variables in this system are not the parameters in others.

There is something to improve the efficiency of the optimization. Even for feasible solutions, the program needs a relatively long time to find solution because of the simulink model inside. We are still finding better and more accurate methods to find optimal solutions.

Structure Subsystem Design – Hao Tan

2.1 Problem Statement

In recent years, increase in gas prices has placed an economic burden on the world. Hence the electric bicycles have been caught increasing attention worldwide, especially in China, Europe and Japan. Electric bikes are a wide range of light vehicles which is very convenient for local transportation. Their silent operation and lack of emissions makes them very suitable for use on bikeways, shared footways and local residential streets.

New bicycle frame designs are generally motivated by weight and/or stiffness considerations and often incorporate the use of high performance engineering materials. (*D. Arola,* 1999) In this project, we will optimize the frame design which involves the topology and mechanical material strength background.

Figure 2 shows the most common structure concept for electrical bicycle frame. (Sheldonbrown, 2008)

Figure 2: Basic frame structure

In order to simplify the problem, we assume the two joint which connect to the wheels to one point. Hence the structure can be shown as Figure 3.

Figure 3: Structure design

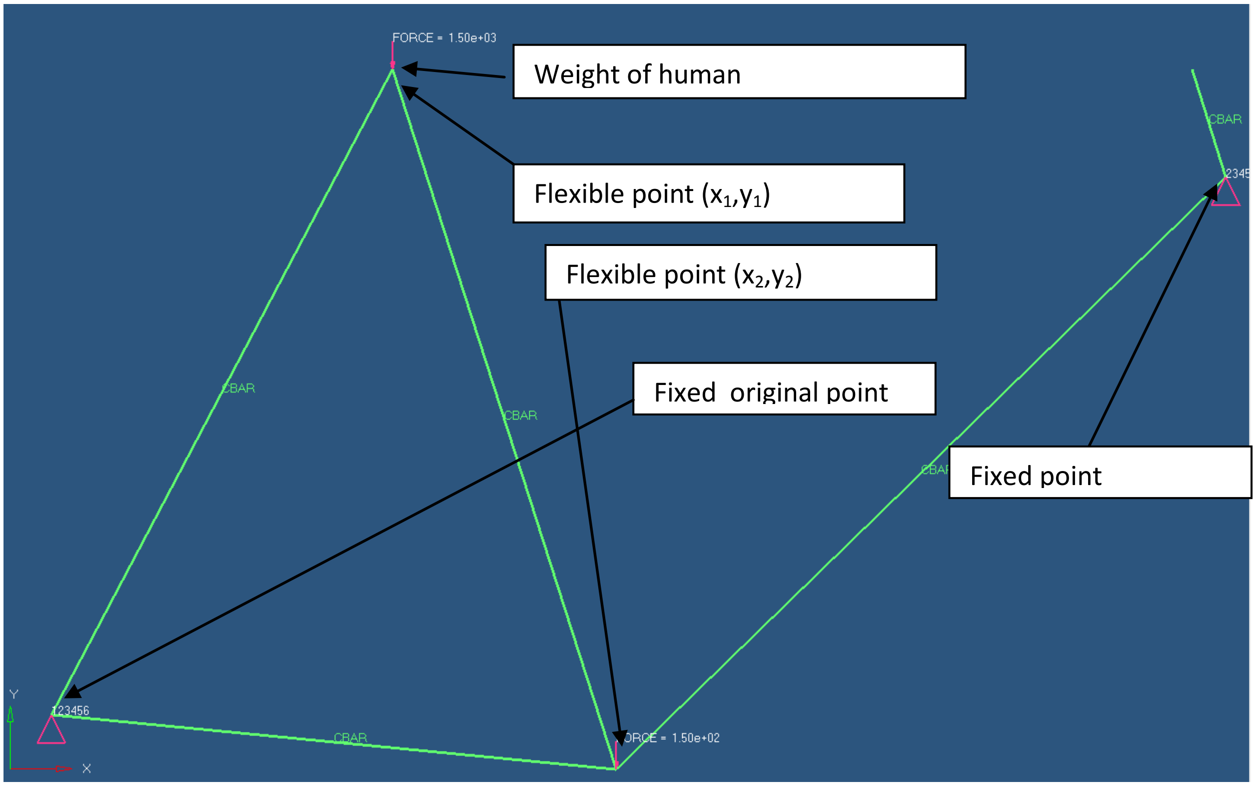

The main problem of this subsystem is to determine an optimal solution for all dimension of the frame, which can stand the load condition without any material fracture and achieve a minimum weight to help the whole system to be more efficient.

2.2 Nomenclature

1. D_i(m)- Outer diameter of the i^{th} beam tube
2. d_i(m)- Inner diameter of the i^{th} beam tube
3. L_i(m)- length of the i^{th} beam tube.
4. ρ(Kg/m^3)- Density of the material.
5. M(Kg)- Mass of the frame.
6. W (N)- Weight of the frame.
8. g(m/s^2)- Gravity acceleration.

9. $\sigma_{b,i}$ (MPa)- Bending stress in the ith member.

10. $\sigma_{a,i}$(MPa)- Axial stress in the ith member.

11. $\sigma_{v,i}$(MPa)- Von Mises stress in the ith member.

12. E (MPa)-- Young's modulus of the material.

13. σ_y(MPa)- Yield stress of the material.

14. FOS- Factor of safety

15. I_i - Moment of inertia for i^{th} beam tube

16. F_{total} (N)- The total load on the frame

17. F_i (N)- The Load on the i^{th} member

18. τ_i(MPa)-- shear stress in the i^{th} member.

19. σ_i (MPa)-- Stress in the i^{th} member.

20. x, y(m)- coordinates

2.3 Mathematical Model

Objective function

The objective function of this subsystem is to minimize the overall weight of the bicycle frame. This will benefit our whole system performance. The objective function can be easily summarized as follow:

$$M = \Sigma \rho\pi(D_i^2 - d_i^2)L_i / 4$$

The *W* represents the total weight of the frame, which is comprised of the weight of each tube in the frame. There are two factors contribute to the weight: the density of material and the total volume of the structure. Usually the material with a light density will be weak in strength; hence the tradeoff is to balance the material's density and its strength.

Constraints

The constraints of this subsystem are consisted from three parts (i) Material properties constraints: The stress in the tube can't make the tube yielding. (ii) Geometry constraints:

some fixed points can't be changed. Also the thickness and length of the all tubes should be in a given range (iii)Load constraints.

First, we determined to focus our optimization on the structure as shown in Figure 3. After this we will focus on the location of all flexible point (as shown in Figure 3), then obtained an equation system which can state the relationship between the flexible point location and maximum stress in the frame. Then we will integrate this equation system with the mechanical material strength equations to build a new system to analysis this subsystem. Finally we will test the Finite Element Analysis result by calculation.

Material properties constraints: In our design optimization we need to ensure the tube con not yield or buckling during the real time using. The following basic solid mechanical equation leads to the final constraints of the system.

$$\sigma_{a,i} = F_N / A_i$$

$$\sigma_{b.i} = MD_i / I$$

$$\sigma_i = \sigma_{a,i} + \sigma_{b.i}$$

$$\sqrt{\sigma_i^2 + 3\tau_i^2} = \sigma_{v,i}$$

$$g1: \sigma_{v,i} - \sigma_y / FOS \leq 0$$

$$g2: F_N \leq \pi EI/(KL)^2$$

Geometry constraints: As we have shown in Figure 3, we added the constraint at the most left and right point in specific direction. Besides that, we assume the thickness of the all tubes should be less than 5mm, which is the common size of bicycle frame manufacture market. The outside diameter of the tube should be between 45 and 50mm. Hence, we can illustrate the constraint as follow:

$$g3: D_i - 0.05 \leq 0$$

$$g4: -D_i + 0.04 \leq 0$$

$$g5: d_i - D_i + 0.001 \leq 0$$

$$g6: D_i - d_i - 0.01 \le 0$$

Load constraints: We assume the weight of human is 90 kg and the total weight of the battery is less than 10 kg. During our FEA analysis, we found the two vertical beams in the left side are the most dangerous tube. So, in order to make our design more safety, we assume all the load of weight is added through the seat to the frame, the condition people just seat on the bicycle. Since we believe under this condition the left two tubes will be the most dangerous, if our design process is under these consideration and assumption, it will be a robust design.

Design variables and parameters

Design variables

- L_i length of the i^{th} beam tube
- D_i Outer diameter of the i^{th} beam tube
- d_i Inner diameter of the i^{th} beam tube

Parameters

- σ_y = 30 MPa Yield stress of the material
- ρ =$2.7*10^3$ Kg/m^3 Density of the material
- E =$69*10^9$ MPa Young's modulus of the material
- F_{total} =900 N The total load on the frame
- FOS =5 Factor of safety

In fact, there are 3*5=15 variables and more than 30 constraints in this subsystem. More constraints will appear in the later process during the model developing.

As we discussed above the must much more constraints will outcome from the software model analysis. The system will become more complex due to the metamodel from the software. Also, there will be some constraints from the battery subsystem which ensure there is enough space for the battery's physical size.

Transformed Model Analysis

The objective function of this subsystem is to minimize the overall weight of the bicycle frame. This will benefit our whole system performance. In our FEA by hypermesh, we assume the uniform properties of the tube cross section and move the flexible point in the given region to obtain the relationship function between the stress and the location of the flexible point. The assumption we made for the software analysis include:

(1)The material of the frame is 6061 aluminum alloy

(2)The safety factor is assigned to be 5.

(3) Properties of the tube cross section are same for every beam.

Figure 4: FEA analysis model

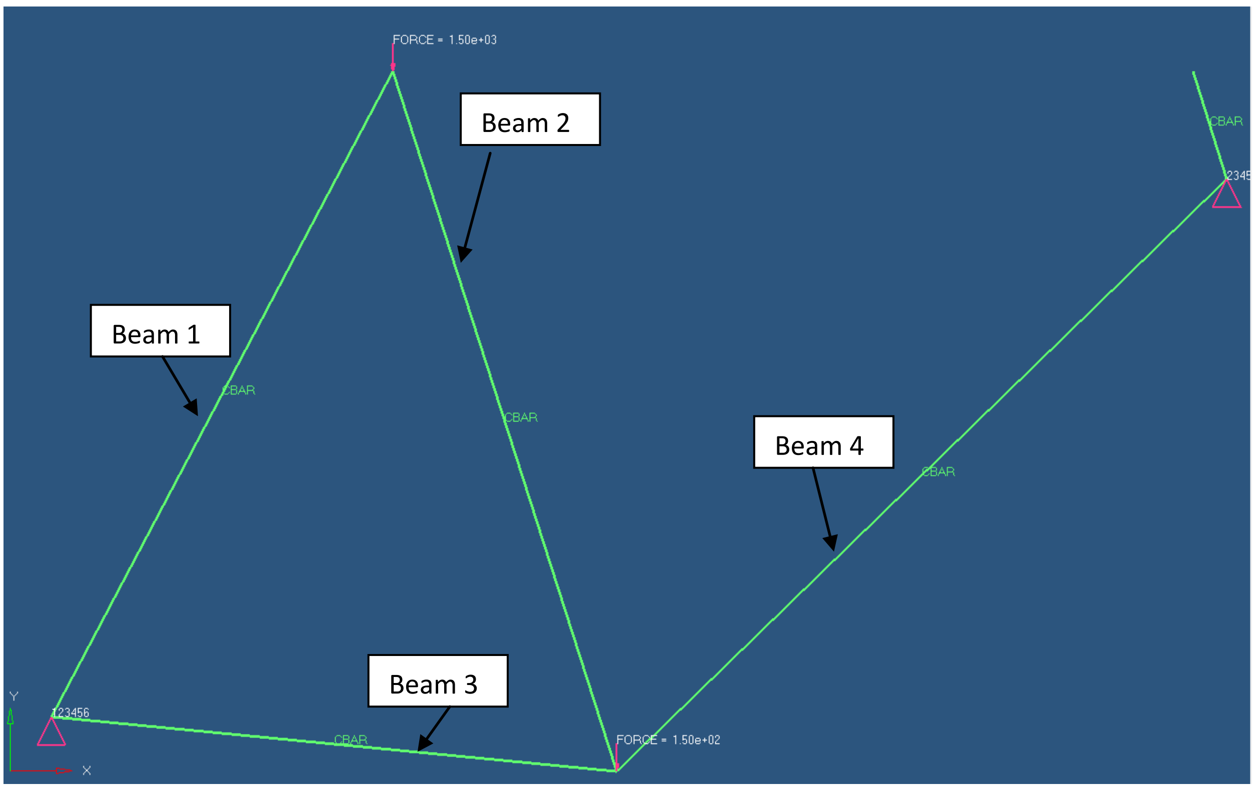

During our FEA analysis, we found that the stress of beam1 and beam2 are always three times of the stress value of beam3 and beam4. Hence, we focused our interesting on dimension of beam1 and beam2. After we find the optimal point of beam1 and beam2, beam3 and beam4 will take the minimum cross section dimension and its length has already determined by the location of flexible point. Also, we found that the axial stress take over 95% contribution of the total stress. So we assume the final stress in these two beams is only determined by the axial stress and ignore the bending stress in the tube.

Free body diagram analysis:

In order to simply the problem, we made a series assumptions as we have discussed above. We use the free body diagram analysis to illustrate the loading on these two beams.

Figure 5: Free body diagram analysis

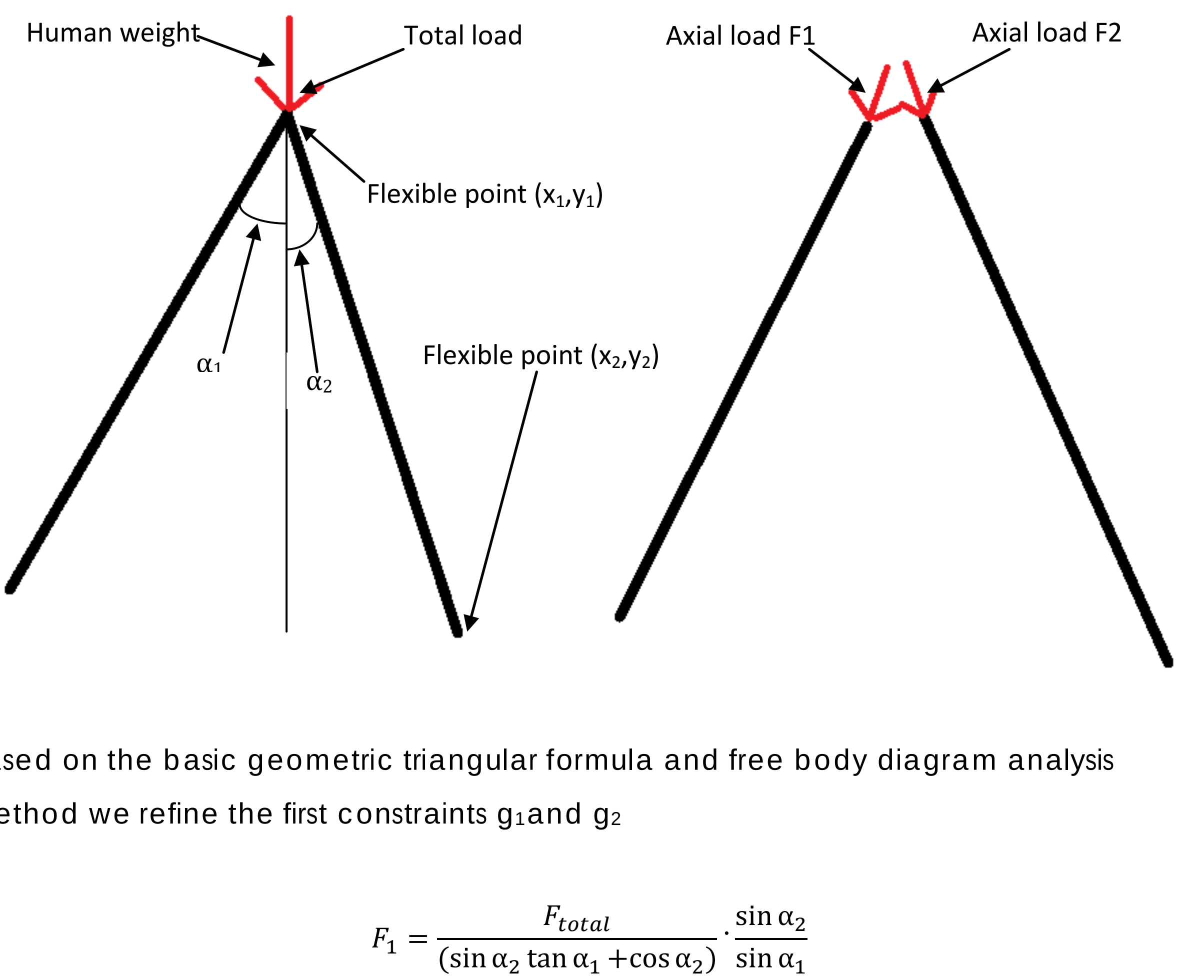

Based on the basic geometric triangular formula and free body diagram analysis method we refine the first constraints $g_1$and g_2

$$F_1 = \frac{F_{total}}{(\sin \alpha_2 \tan \alpha_1 + \cos \alpha_2)} \cdot \frac{\sin \alpha_2}{\sin \alpha_1}$$

$$F_2 = \frac{F_{total}}{(\sin \alpha_2 \tan \alpha_1 + \cos \alpha_2)}$$

$$\tan \alpha_1 = \frac{x_1}{y_1}$$

$$\sin \alpha_1 = \frac{x_1}{\sqrt{(x_1^2 + y_1^2)}}$$

$$\cos \alpha_1 = \frac{y_1}{\sqrt{(x_1^2 + y_1^2)}}$$

$$\sin \alpha_2 = \frac{x_2 - x_1}{\sqrt{(x_1 - x_2)^2 + (y_1 - y_2)^2}}$$

$$\cos \alpha_2 = \frac{y_1 - y_2}{\sqrt{(x_1 - x_2)^2 + (y_1 - y_2)^2}}$$

Finally, the simplified mathematical model is:

Objective function:

$$minmize \qquad M = \frac{\pi}{4} \cdot \rho \cdot ((D_1^2 - d_1^2) \cdot \sqrt{(x_1^2 + y_1^2)} + (D_2^2 - d_2^2) \cdot \sqrt{(x_1 - x_2)^2 + (y_1 - y_2)^2)})$$

Subject to:

g_1: $\frac{3600}{(\sin \alpha_2 \tan \alpha_1 + \cos \alpha_2)} \cdot \frac{\sin \alpha_2}{\sin \alpha_1} - \frac{30}{5} * 10^6 * \pi * (D_1^2 - d_1^2) \leq 0$

g_2: $\frac{3600}{(\sin \alpha_2 \tan \alpha_1 + \cos \alpha_2)} - 30/5 * 10^6 * \pi * (D_2^2 - d_2^2) \leq 0$

g_3: $D_1 - 0.05 \leq 0$

g_4: $-D_1 + 0.04 \leq 0$

g_5: $D_2 - 0.05 \leq 0$

g_6: $-D_2 + 0.04 \leq 0$

g_7: $d_1 - D_1 + 0.001 \leq 0$

g_8: $D_1 - d_1 - 0.01 \leq 0$

g_9: $d_2 - D_2 + 0.001 \leq 0$

g_{10}: $D_2 - d_2 - 0.01 \leq 0$

g_{11}: $0.5 - \sqrt{(x_1 - x_2)^2 + (y_1 - y_2)^2} \leq 0$

g_{12}: $\sqrt{(x_1^2 + y_1^2)} - 0.6 \leq 0$

g_{13}: $0.45 - \sqrt{(x_1^2 + y_1^2)} \leq 0$

g_{14}: $\sqrt{(x_1 - x_2)^2 + (y_1 - y_2)^2} - 0.6 \leq 0$

g_{15}: $0.194 - x_1 \leq 0$

g_{16}: $x_1 - 0.294 \leq 0$

g_{17}: $0.411 - y_1 \leq 0$

g_{18}: $y_1 - 0.511 \leq 0$

g_{19}: $0.364 - x_2 \leq 0$

g_{20}: $x_2 - 0.444 \leq 0$

g_{21}: $-0.043 - y_2 \leq 0$

g_{22}: $y_2 + 0.035 \leq 0$

g_{23}: $\frac{900}{(\sin\alpha_2 \tan\alpha_1 + \cos\alpha_2)} \cdot \frac{\sin\alpha_2}{\sin\alpha_1} - \frac{69*10^9*\pi^3*(D_1^4 - d_1^4)}{256*(x_1^2+y_1^2)} \leq 0$

g_{24}: $\frac{900}{(\sin\alpha_2 \tan\alpha_1 + \cos\alpha_2)} - \frac{69*10^9*\pi^3*(D_2^4 - d_2^4)}{256*((x_1-x_2)^2+(y_1-y_2)^2)} \leq 0$

2.4 Model Analysis

After we simplify our model for this subsystem, we conducted the monotonicity analysis to improve our mathematical model.

Monotonicity analysis

Table1: Monotonicity analysis table

	D_1	d_1	D_2	d_2	x_1	y_1	x_2	y_2
f	+	-	+	-	+	+	-	-
g_1	-	+			U	U	U	U
g_2			-	+	U	U	U	U
g_3	+							
g_4	-							
g_5			+					
g_6			-					
g_7	-	+						
g_8	+	-						
g_9			-	+				
g_{10}			+	-				

g_{11}					-	-	+	+
g_{12}					+	+		
g_{13}					-	-		
g_{14}					+	+	-	-
g_{15}					-			
g_{16}					+			
g_{17}						-		
g_{18}						+		
g_{19}							-	
g_{20}							+	
g_{21}								-
g_{22}								+
g_{23}	-	+			U	U	U	U
g_{24}			-	+	U	U	U	U

Discussion for monotonicity analysis:

Based on the monotonicity analysis table in the previous page makes the following points clear,

1. The objective function (mass) is a heavily monotonic function of the design variables. This is common problem in structural engineering. Notice that the mass is found to increase with the outer diameter D_i and the lengths l_i of all tubes, the mass also decrease respect to the inner diameter d_i. It is very easy to see based on common sense. The outer diameter D_i and the lengths l_i are the positive monotonic variables. The inner diameter d_i is negatively monotonic variable of objective function.
2. The constraints *g3, g5, g8, g10, g12, g14* can be deleted by the MP1 theorem.
3. Since we have already defined a feasible region based on the knowledge and com common sense, all variables are well bounded.

After the discussion, we can simplify our model again. The reduced monotonicity analysis table is shown in table 2. Now, our model has 8 variable and 18 constraints.

Table2: Reduced monotonicity analysis table

	D_1	d_1	D_2	d_2	x_1	y_1	x_2	y_2
f	+	-	+	-	U	U	U	U
g_1	-	+			U	U	U	U
g_2			-	+	U	U	U	U
g_4	-							
g_6			-					
g_7	-	+						
g_9			-	+				
g_{11}					-	-	+	+
g_{13}					-	-		
g_{15}					-			
g_{16}					+			
g_{17}						-		
g_{18}						+		
g_{19}							-	
g_{20}							+	
g_{21}								-
g_{22}								+
g_{23}	-	+			U	U	U	U
g_{24}			-	+	U	U	U	U

2.5 Numerical Results

In this section, we show our final optimal result. The calculation is completed by the excel solver and fmincon function in the Matlab. The excel solver is based on the GRG (Generalized Reduced Gradient) nonlinear optimization codes. The Matlab uses SPQ algorithm. After we simplified our model, we reform it and then obtained the final optimal point in the feasible region. Table 3 shows the final result. Detail information is in the Appendix A.4.

Table 3: Optimal result

	Initial point	Optimal point 1	Initial point2	Optimal point 2	Initial point 3	Optimal point 3
f	4.96	3.86	3.59	3.86	4.96	3.86
$D_1\ (m)$	0.045	0.0400	0.045	0.0400	0.05	0.040
$d_1(m)$	0.043	0.0390	0.043	0.0390	0.048	0.039
$D_2(m)$	0.045	0.0459	0.040	0.0400	0.05	0.0437
$d_2(m)$	0.043	0.0440	0.039	0.0377	0.048	0.0417
$x_1(m)$	0.244	0.294	0.244	0.294	0.214	0.294
$y_1(m)$	0.461	0.511	0.461	0.511	0.421	0.511
$x_2(m)$	0.404	0.435	0.404	0.435	0.364	0.435
$y_2(m)$	-0.039	-0.035	-0.039	-0.035	-0.043	-0.035

For the first and third initial point, the optimal shows that it saves more than 20% in the total weight of the bicycle frame. The second initial point is not in the feasible domain, the constraint *g1* can't be satisfied at this initial point. Hence, the optimal doesn't appear a reduction of the objective function.

The different initial points share the same optimal vale of location of two flexible points and cross section dimension of the first tube. The inner and outer diameter of the second tube are various, the final optimal values of the objective function are same. The reason behind these results could be the active nonlinear constraint, which can give us multiple optimal points. Obviously, these optimal points are just local optimal point. Since the final objective function value is same for these optimal points, they must be located on the same gradient line of the objective function. Also, we noticed that the different optimal results share the same area of cross section. It is reasonable, since the area determine the axial stress as well as the volume under a given length of the tube.

The location of the two flexible points has already reached at its corresponding boundary of feasible region. It means we may need to recheck the feasible region constraints by involved more consideration and discussion of ergonomics analysis or manufacturability condition.

Table 4: Result report of constraints

Cell	Name	Cell Value	Formula	Status	Slack
B13	g1	0	B13<=0	Binding	0
B14	g2	2.32484E-07	B14<=0	Binding	0
B15	g3	-0.01	B15<=0	Not Binding	0.01
B16	g4	0	B16<=0	Binding	0
B17	g5	-0.004002624	B17<=0	Not Binding	0.004002624
B18	g6	-0.005997376	B18<=0	Not Binding	0.005997376
B19	g7	0	B19<=0	Binding	0
B20	g8	-0.009	B20<=0	Not Binding	0.009
B21	g9	-0.000905999	B21<=0	Not Binding	0.000905999
B22	g10	-0.008094001	B22<=0	Not Binding	0.008094001
B23	g11	-0.064009004	B23<=0	Not Binding	0.064009004
B24	g12	-0.010460349	B24<=0	Not Binding	0.010460349
B25	g13	-0.139539651	B25<=0	Not Binding	0.139539651
B26	g14	-0.035990996	B26<=0	Not Binding	0.035990996
B27	g15	-0.1	B27<=0	Not Binding	0.1
B28	g16	0	B28<=0	Binding	0
B29	g17	-0.1	B29<=0	Not Binding	0.1
B30	g18	0	B30<=0	Binding	0
B31	g19	-0.07138655	B31<=0	Not Binding	0.07138655
B32	g20	-0.00861345	B32<=0	Not Binding	0.00861345
B33	g21	-0.008	B33<=0	Not Binding	0.008
B34	g22	0	B34<=0	Binding	0
B33	g21	-0.008	B33<=0	Not Binding	0.008
B34	g22	0	B34<=0	Binding	0
B35	g23	-5555.827017	B35<=0	Not Binding	5555.827017
B36	g24	-17503.3391	B36<=0	Not Binding	17503.3391

Table 5: Sensitivity report of constraint

Cell	Name	Final Value	Lagrange Multiplier
B13	g1	0	0.00569164
B14	g2	2.32484E-07	0.0030896
B15	g3	-0.01	0
B16	g4	0	0.00116927
B17	g5	-0.004002624	0
B18	g6	-0.005997376	0
B19	g7	0	0.045601686
B20	g8	-0.009	0
B21	g9	-0.000905999	0
B22	g10	-0.008094001	0
B23	g11	-0.064009004	0
B24	g12	-0.010460349	0
B25	g13	-0.139539651	0
B26	g14	-0.035990996	0
B27	g15	-0.1	0
B28	g16	0	5.13189E-06
B29	g17	-0.1	0
B30	g18	0	0.00027137
B31	g19	-0.07138655	0
B32	g20	-0.00861345	0
B33	g21	-0.008	0
B34	g22	0	0.000178792
B35	g23	-5555.827017	0
B36	g24	-17503.3391	0

From Table 4, we noticed that the *g1, g2, g4, g7, g16, g18, g22* are the active constraint, with a final value of 0 and "binding" indicator. In Table 5, we found that all the active constraints have a positive Lagrange Multiplier.

$$g_1: \frac{3600}{(\sin\alpha_2 \tan\alpha_1 + \cos\alpha_2)} \cdot \frac{\sin\alpha_2}{\sin\alpha_1} - 30/5 * \pi * (D_1^2 - d_1^2) = 0$$

$$g_2: \frac{3600}{(\sin\alpha_2 \tan\alpha_1 + \cos\alpha_2)} - 30/5 * \pi * (D_2^2 - d_2^2) = 0$$

$$g_4: -D_1 + 0.04 = 0$$

$$g_7: d_1 - D_1 + 0.001 = 0$$

$$g_{16}: x_1 - 0.294 = 0$$

$$g_{18}: y_1 - 0.511 = 0$$

$$g_{22}: y_2 + 0.035 = 0$$

From *g4 and g7, we can determine* D_1 *and* d_1. *Based on g16, g18, g22 we can easily find the optimal solution of the flexible point:*

$$D_1 = 0.04$$

$$d_1 = 0.039$$

$$x_1 = 0.294$$

$$y_1 = 0.511$$

$$y_2 = -0.035$$

These results also agree with the monotonicity analysis table as shown in table 1 and 2.

2.6 Parametric Studies

In this part, we try to analysis some parameters of our model to find some sensitivity parameters. Obviously, the first two constraints are very critical to this subsystem design. From our optimal result we found that, these two constraints are always active. These constraints are determined by the material yield stress and safety factor.

$$g_1: \frac{3600}{(\sin\alpha_2 \tan\alpha_1 + \cos\alpha_2)} \cdot \frac{\sin\alpha_2}{\sin\alpha_1} - \frac{30}{5} * 10^6 * \pi * (D_1^2 - d_1^2) \leq 0$$

$$g_2: \frac{3600}{(\sin\alpha_2 \tan\alpha_1 + \cos\alpha_2)} - \frac{30}{5} * 10^6 * \pi * (D_2^2 - d_2^2) \leq 0$$

In our current model, the material yield stress is 30MPa which is the average of 6061 aluminum; the safety factor is assigned to be 5. Table 6 shows some different optimal result respect to varied combination of material yield stress and safety factor.

From our result section, we noticed that the last two constraints, *g23* and *g24,* are inactive, which are derived from the buckling constraint we discussed in the model section. The actual force in our model is just about 2% of the critical buckling load. It means that we don't need to worry about the buckling problem in our design problem. Hence, we just discuss about the parameter of the yield stress and safety factor.

Table 6: Parameter analysis

		Optimal point			
	Initial point	Original case	Case I	Case II	Case III
σ_y/FOS (MPa)	6	6	3	9	2.2
f	4.96	3.86	6.04	2.99	No solution
$D_1\,(m)$	0.045	0.0442	0.0400	0.0448	
$d_1(m)$	0.043	0.0437	0.0389	0.0445	
$D_2(m)$	0.045	0.0459	0.0400	0.0437	
$d_2(m)$	0.043	0.0439	0.0352	0.0423	
$x_1(m)$	0.244	0.294	0.294	0.294	
$y_1(m)$	0.461	0.511	0.511	0.511	
$x_2(m)$	0.404	0.435	0.435	0.435	
$y_2(m)$	-0.039	-0.035	-0.035	-0.035	

From table 6 we can see that the ratio between material yield stress and safety factor (σ_y/FOS) is very important to the final result. For case I and II, the location of the flexible point is same but the objective function value has a big difference. It means that in the given feasible region the best location is same if the ratio between material yield stress and safety factor in some fixed range. Also, if this ratio is too small, we can't find a solution in the given feasible region. The final objective function value decreases with the increasing of ratio (σ_y/FOS). It easy to understand, under same safety factor, the stronger material will have a lighter weight.

From these result and analysis, we noticed that the material selection and definition of the feasible region are very critical to the final optimal solution. In further study of this problem, we must be more careful to these parameters

2.7 Discussion of Results

In this section, we will discuss about our numerical results and translate them to a real time physical meaning.

From table 3, we found that the location of the optimal points is uniform for different initial points.

$$x_1 = 0.294m$$

$$y_1 = 0.511m$$

$$x_2 = 0.435m$$

$$y_2 = -0.035m$$

For the location, we realized that three of them already reach the boundary of the feasible region which was given by the assumption in our model analysis section. Since we don't want to change the topology structure of the frame, our assumption of the feasible region for the flexible point is not very huge.

Figure 6: Final location of flexible point

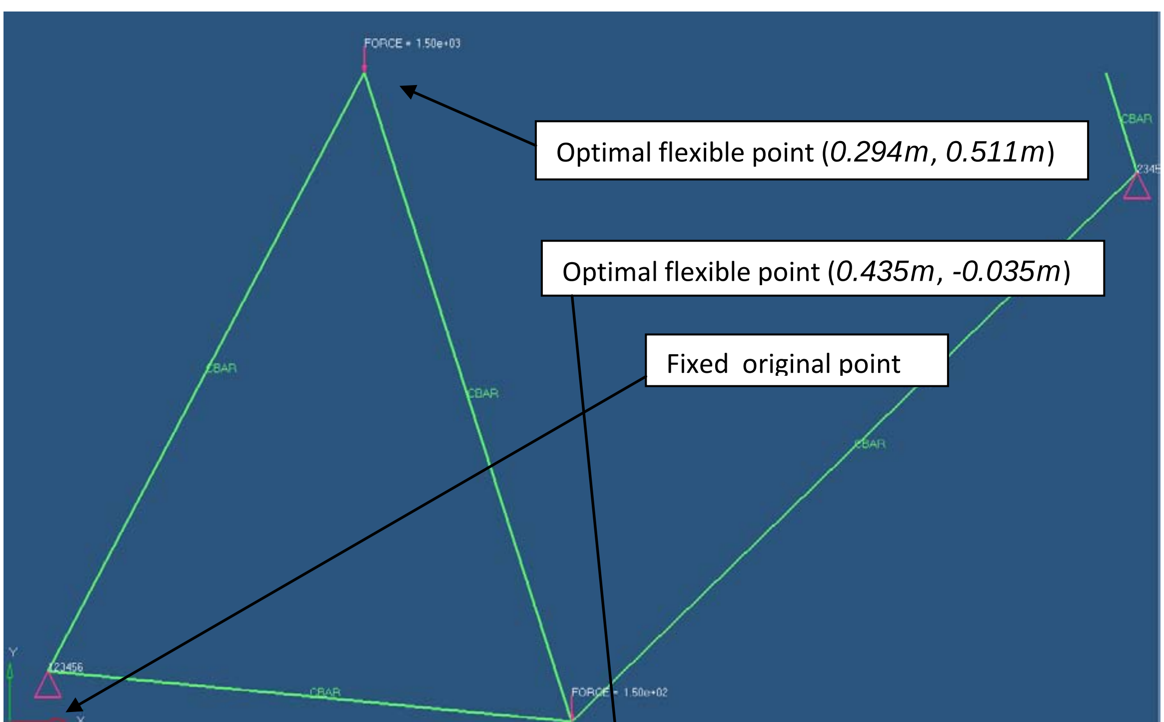

The dimension of the tubes is determined by the inner and outer diameter and the location of flexible point. The final dimensions of these four tubes are shown in table 7.

Table 7: Final result

	Beam1	Beam 2	Beam 3	Beam 4
Length(m)	0.590	0.564	0.436	0.582
Outer diameter D (m)	0.0400	0.0459	0.0400	0.0400
Inner diameter d(m)	0.0390	0.0440	0.0390	0.0390

The final objective function stands for the total mass of the material (6061 aluminum alloy, the total weight of our optimal frame design is 4.64Kg, while the initial weight of the frame is 6.61Kg.

The main goal of this subsystem is to reduce weight of the frame, which can stand the load condition without any material fracture. Smaller the area of the cross section will leads to a lighter weight of the frame, but it become more dangerous for the tube at same time. The further study may focus on the consideration and discussion of ergonomics analysis or manufacturability condition, since it may redefine the feasible region of the design variable and improve the system's performance.

3. SYSTEM INTEGRATION STUDY

In this section, the subsystem problems are integrated to form the entire electric-bicycle design optimization problem. It should be recalled so far the optimization study has been performed individually on four subsystems: (1) Battery, (2) Motor, (3) Motor controller, and (4) Structure. Each system has a specific objective and a set of design variables and parameters. The individual subsystem optimization is based on the assumption that the parameter values for each problem are well-known and remain constant throughout the optimization process. However, some of these parameters are actually highly dependent on other subsystem. For example, in the motor controller subsystem, two parameters: motor resistance (R_a) and motor moment of inertia (J_a) are given constant values when analyzing this subsystem alone. But these two quantities are in fact functions of the design variables of motor subsystem (L_{wa}, D, d_s):

$$R_a = \frac{\rho L_{wa}}{4A_{wa}}$$

$$J_a = 0.5\rho_{Fe} L\pi(\frac{D}{2} - d_s)^2 - 0.5\rho_{Cu} L_{wa} A_{wa}\left[\left(\frac{D}{2}\right)^2 - \left(\frac{D}{2} - d_s\right)^2\right]$$

Therefore, when the subsystems are integrated together, L_{wa}, D, d_s are the linking (common) variables between the motor and motor controller subsystems. Another example is in the structure subsystem, the loading force (F_{total}), or in other words, the weight of the battery (W_{bat}) is treated as a constant. However, it depends on the number of cells within the battery (n_{cel}). Thus n_{cel} becomes the linking variable between the structure and battery subsystem.

Another reason to perform system integration optimization is that there exist design trade-offs among the subsystem design objectives. In other words, the overall objective of entire system cannot be achieved by simply arriving at optimal solutions for all the subsystems. Specifically, the overall objective of the entire electric bicycle system is to minimize the overall weight, including the weight of battery, motor and structure beams. In the battery subsystem, the objective is to maximize the power efficiency, which requires the number of cells to be carefully designed (thus the battery weight) to achieve this maximum efficiency. However, there is no guarantee that the battery weight will be at minimum because the efficiency also depends on the power command from motor subsystem.

Another important design conflict is the power supply of the battery and motor versus the structure loading. As discussed in the subsystem analysis, as the number of batteries used increases, more power will be provided. But this also increases the weight of the battery. Similarly, as we increase the power demand in the motor, the weight of the motor also increases because longer armature wire will be needed to ensure the safety power level. As the weight of battery and motor increases, more loading force and torque are applied to the bicycle structure, which will cause the stress within the beam structures to increase. Thus this design trade-off is important to ensure safety for the mechanical structure during riding.

The entire system design optimization problem is shown schematically in Figure 3.1 below:

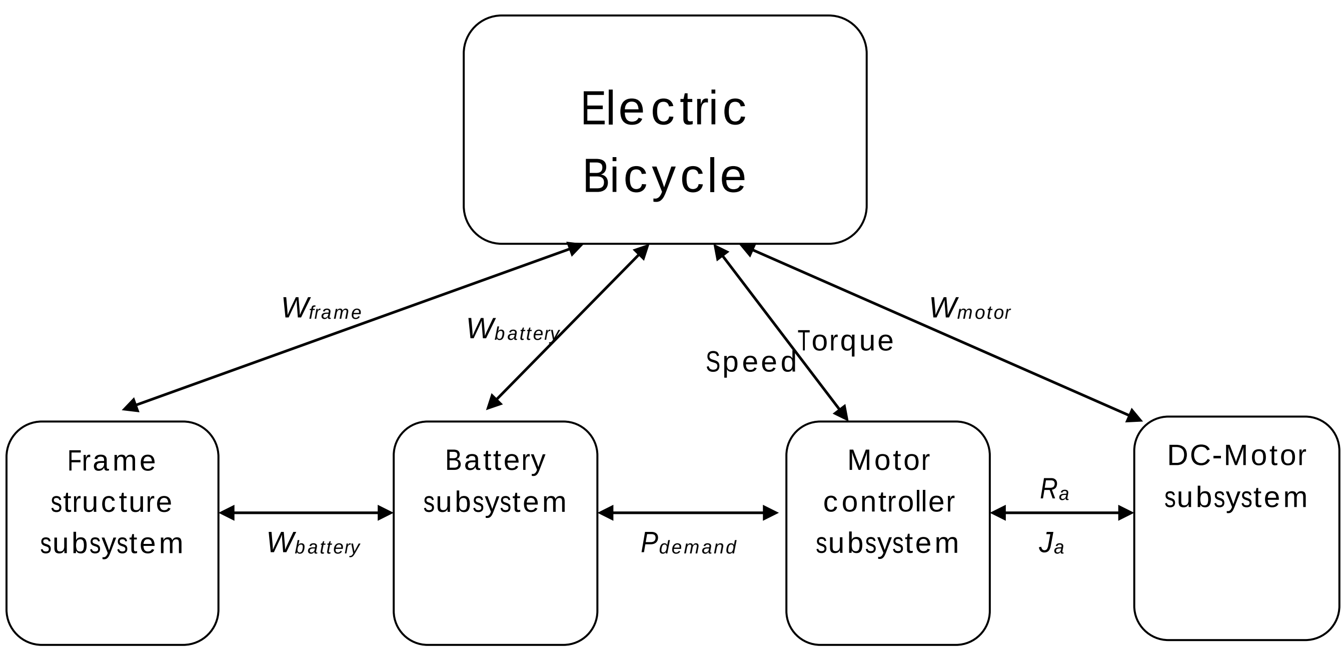

Figure 3.1: Schematic diagrams of entire electric bicycle system

3.1 Objective Function

Based on the above discussion, the system integration is done by forming the system problem into a single optimization problem, which is the so-called All-In-One (AIO) approach. The system objective is to minimize the weight of the entire structure, including the weight of battery, motor and structure beams:

$$\text{Minimize } f = W_{mot} + W_{bat} + W_{str}$$

Here, W_{mot}, W_{bat}, and W_{str} represent the total weight of the motor, the total weight of the battery, and the total weight of the bicycle structure beams. By substituting in the definitions from each subsystem, the objective function can be written in a more detailed format as:

$$\begin{aligned} f &= \rho_{Cu}(A_{wa}L_{wa} + A_{wf}L_{wf}) + \rho_{Fe}L\pi(D + d_s)^2 + n_{cel}W_{cel} \\ &+ \rho_{Al}\frac{\pi}{4}\left[\left(D_1^2 - d_1^2\right)\sqrt{\left(x_1^2 + y_1^2\right)} + \left(D_2^2 - d_2^2\right)\sqrt{\left(x_1 - x_2\right)^2 + \left(y_1 - y_2\right)^2}\right] \end{aligned}$$

3.2 Constraints

The constraints of the overall electric bicycle system are composed of: (1) constraints from original individual subsystems, (2) the linking constraints showing the trade-offs among subsystems, and (3) Original subsystem objective functions now serving as the constraints of the overall system (This applies to the battery and motor controller subsystem). The following discussion details these added constraints to the overall system.

First of all, two equality constraints are added to the problem based on:

$$h_1 = R_a - \frac{\rho L_{wa}}{4A_{wa}} = 0$$

$$h_2 = J_a - \left(0.5\rho_{Fe} L\pi(\frac{D}{2} - d_s)^2 - 0.5\rho_{Cu} L_{wa} A_{wa} \left[\left(\frac{D}{2}\right)^2 - \left(\frac{D}{2} - d_s\right)^2 \right] \right) = 0$$

These two equations give the connection between motor subsystem and the motor controller subsystem. In the motor subsystem, the variable L_{wa}, L, D, d_s are determined through optimization study. The results also determine the value of armature resistance (R_a) and motor moment of inertia (J_a), which will be used in the motor controller subsystem.

Secondly, the linking variable between the battery subsystem and the structure subsystem is the number of cells in the battery (n_{cel}), which is given as:

$$F_{tot} - (W_{user} + n_{cel} W_{cel} g) = 0$$

Here, the F_{tot} is the total weight applied in the frame beam, which is assumed to be the weight of a normal person (W_{user} = 900N). In fact, as a system point of view, the weight of the battery should also be taken into account.

Another thing to mention is that in the original battery optimization sub-problem, the battery efficiency is assumed to be constant (90%). However, at a system level, it is more reasonable to provide upper and lower bounds of the efficiency (70%-100%). This change is reflected in constraints g_{56} and g_{57} in the summary model.

3.3 Design Variables and Parameters

The design variables and parameters for the integrated system are summarized in table 3.3.1 and 3.3.2 below:

Table 3.3.1: List of design variables

Symbols	Description	Units
D	Rotor diameter	m
D_i	Outer diameter of the ith beam tube	m
d_i	Inner diameter of the ith beam tube	m
d_s	Depth of slots	m
I_{bat}	Battery output current	A
J_a	Motor moment of inertia	kg·m^2
k_d	Derivative gain	N/A
k_i	Integral gain	N/A
k_p	Proportional gain	N/A
L	Rotor axial length	m
L_{wa}	Length of armature wire	m
L_{wf}	Length of field wire	m
n_{cel}	Battery cell number	1
R_a	Armature resistance	Ω
T	Battery working temperature	^{o}C
x_i	x position of the ith flexible	m
y_i	y position of the ith flexible	m

Table 3.3.2: List of design parameters

Symbols	Description	Values	Units
A_{wa}	Cross-section area of armature wire	2×10^{-6}	m^2
A_{wf}	Cross-section area of field wire	1×10^{-6}	m^2
a	Number of parallel paths	5	1
B	Rolling resistance	0.01	N·s/m
b_{fc}	Depth of field coil	0.045	m
C_{lim}	Battery capacity limit	280	Wh/kg
D_{bat}	Specific volume energy	115	Wh/l
f_{cf}	Copper space factor	0.65	1

g	Acceleration of gravity	9.81	m/s^2
K_t	Torque constant	5	N·m/A
K_v	Back-emf constant	0.3	V·s/rad
L_a	Armature inductance	0.5	H
I_{ul}	battery current upper limit	10	A
n_d	Rotational speed	24	rad/s
n_{lim}	Number of cells limits	14	1
p	Number of poles	2	1
P_{mind}	Minimum required power	0.67	kW
R_{bat}	Battery total resistance	0.3	Ω
S	Number of slots or teeth on rotor	10	1
t	Simulation time	30	sec
T_{env}	Environmental temperature	23	^oC
T_{load}	Load torque	1	N·m
T_{max}	Maximum battery temperature	50	^oC
T_{min}	Minimum battery temperature	-20	^oC
W_{cel}	Weight per battery cell	0.3	kg
W_{user}	Weight of the user	900	N
η	Motor efficiency	85%	1
η_{bat}	Battery energy efficiency	90%	1
ρ	Resistivity of copper wires	1.68×10^{-8}	Ω·m
ρ_{Al}	Density of aluminum	2700	kg/m^3
ρ_{Cu}	Density of copper	8900	kg/m^3
ρ_{Fe}	Density of iron	7900	kg/m^3

After substituting the numerical values for the design parameters, the entire system model is summarized in standard negative null form as in the summary model on next page.

3.4 Summary Model

$$\min\ f = 0.0178L_{wa} + 0.0089L_{wf} + 24818.58L(D+d_s)^2 + 0.3n_{cel} +$$

$$2120\left[\left(D_1^2 - d_1^2\right)\sqrt{\left(x_1^2 + y_1^2\right)} + \left(D_2^2 - d_2^2\right)\sqrt{\left(x_1 - x_2\right)^2 + \left(y_1 - y_2\right)^2}\right]$$

Subject to:

$$h_1 = R_a - 0.0021L_{wa} = 0$$

$$h_2 = J_a - \left(12409.3L\left(\frac{D}{2} - d_s\right)^2 - 0.0089L_{wa}\left(D - d_s\right)d_s\right) = 0$$

$$g_1 = -L_{wa} \le 0$$

$$g_2 = -L_{wf} \le 0$$

$$g_3 = -L \le 0$$

$$g_4 = -D \le 0$$

$$g_5 = -d_s \le 0$$

$$g_6 = D - 0.241916 \le 0$$

$$g_7 = L - 1.413717D \le 0$$

$$g_8 = 0.942478D - L \le 0$$

$$g_9 = d_s - 0.2142857D \le 0$$

$$g_{10} = -d_s + 0.1D \le 0$$

$$g_{11} = d_s - 0.278431D \le 0$$

$$g_{12} = d_s - 0.5D \le 0$$

$$g_{13} = L_{wa} - 9565.446LD - 17279.17D^2 - 23913.62d_sD \le 0$$

$$g_{14} = -L_{wa} + 2869.634LD + 5183.752D^2 + 7174.085d_sD \le 0$$

$$g_{15} = L_{wa} - (2617994L + 4729185D + 6544985d_s)(Dd_s - d_s^2) \le 0$$

$$g_{16} = 18.715L^3 + 5.895L^2 + 0.606L + 0.02 - L^3L_{wf} \le 0$$

$$g_{17} = -93.574L^3 - 29.476L^2 - 3.032L - 1.029 + L^3 L_{wf} \leq 0$$

$$g_{18} = T - 50 \leq 0$$

$$g_{19} = 10 - T \leq 0$$

$$g_{20} = I_{bat} - 10 \leq 0$$

$$g_{21} = 0.1 - I_{bat} \leq 0$$

$$g_{22} = 13 - n_{cel}\left(3.6 - I_{bat}\left(8\times10^{-8}T^4 - 10^{-5}T^3 + 0.0006T^2 - 0.0181T + 0.2735\right)\right) \leq 0$$

$$g_{23} = n_{cel}\left(3.6 - I_{bat}\left(8\times10^{-8}T^4 - 10^{-5}T^3 + 0.0006T^2 - 0.0181T + 0.2735\right)\right) - 50 \leq 0$$

$$g_{24} = 9\times10^{-8}T^4 - 2\times10^{-6}T^3 - 0.0005T^2 + 0.0282T + 0.8861 - 1.5 \leq 0$$

$$g_{25} = 1.1 - \left(9\times10^{-8}T^4 - 2\times10^{-6}T^3 - 0.0005T^2 + 0.0282T + 0.8861\right) \leq 0$$

$$g_{26} = \left(9\times10^{-8}T^4 - 2\times10^{-6}T^3 - 0.0005T^2 + 0.0282T + 0.8861\right)n_{cel} - 40 \leq 0$$

$$g_{27} = 1.1 - \left(9\times10^{-8}T^4 - 2\times10^{-6}T^3 - 0.0005T^2 + 0.0282T + 0.8861\right)n_{cel} \leq 0$$

$$g_{28} = n_{cel} - 15 \leq 0$$

$$g_{29} = 0 - n_{cel} \leq 0$$

$$g_{30} = 4\left(2.94n_{cel} + 900\right)y_1\left(x_2 - x_1\right)\sqrt{x_1^2 + y_1^2} - 18.85\times10^6\left(D_1^2 - d_1^2\right)x_1^2\left(y_1 - y_2\right) \leq 0$$

$$g_{31} = 4\left(2.94n_{cel} + 900\right)y_1\left(x_2 - x_1\right)\sqrt{\left(x_1 - x_2\right)^2 + \left(y_1 - y_2\right)^2} - 18.85\times10^6\left(D_2^2 - d_2^2\right)\left(x_1x_2 - x_1^2\right)\left(y_1 - y_2\right) \leq 0$$

$$g_{32} = D_1 - 0.05 \leq 0$$

$$g_{33} = -D_1 + 0.04 \leq 0$$

$$g_{34} = D_2 - 0.05 \leq 0$$

$$g_{35} = -D_2 + 0.04 \leq 0$$

$$g_{36} = d_1 - D_1 + 0.001 \leq 0$$

$$g_{37} = -d_1 + D_1 - 0.01 \leq 0$$

$$g_{38} = d_2 - D_2 + 0.001 \leq 0$$

$$g_{39} = -d_2 + D_2 - 0.01 \leq 0$$

$$g_{40} = 0.25 - \left(x_1 - x_2\right)^2 - \left(y_1 - y_2\right)^2 \leq 0$$

$$g_{41} = x_1^2 + y_1^2 - 0.36 \le 0$$

$$g_{42} = -\left(x_1^2 + y_1^2\right) + 0.2025 \le 0$$

$$g_{43} = \left(x_1 - x_2\right)^2 + \left(y_1 - y_2\right)^2 - 0.36 \le 0$$

$$g_{44} = 0.194 - x_1 \le 0$$

$$g_{45} = x_1 - 0.294 \le 0$$

$$g_{46} = 0.411 - y_1 \le 0$$

$$g_{47} = y_1 - 0.511 \le 0$$

$$g_{48} = 0.366 - x_2 \le 0$$

$$g_{49} = x_2 - 0.444 \le 0$$

$$g_{50} = -0.043 - y_2 \le 0$$

$$g_{51} = y_2 + 0.035 \le 0$$

$$g_{52} = M_p - 35\% \le 0$$

$$g_{53} = -M_p \le 0$$

$$g_{54} = t_s - 5 \le 0$$

$$g_{55} = -t_s \le 0$$

$$g_{56} = I_{bat}\left(9\times10^{-8}T^4 - 2\times10^{-6}T^3 - 0.0005T^2 + 0.0282T + 0.8861\right) - 1.08 \le 0$$

$$g_{57} = -I_{bat}\left(9\times10^{-8}T^4 - 2\times10^{-6}T^3 - 0.0005T^2 + 0.0282T + 0.8861\right) \le 0$$

Number of design variables: *21*

Number of equality constraints: 2

Number of inequality constraints: 57

Degree of freedom (DOF): 19

3.5 Numerical Results

The system optimization results are obtained numerically by using MATLAB fuction "fmincon". The optimal solution is shown below in Table 3.5.1. The results obtained from individual subsystem optimization are also presented in this table for comparison purpose.

Table 3.5.1: Optimal solutions for integrated system vs. subsystem

Symbols	Integrated system results	Subsystem results
W	12.25	11.8
L_{wa}	97.76605	14.84918
L_{wf}	231.3784	452.9633
L	0.078707	0.0545918
D	0.055674	0.038616
d_s	0.005567	0.0038616
n_{cel}	3.22	3.66
D_1	0.04	0.04
D_2	0.04	0.0459
d_1	0.039	0.039
d_2	0.039	0.044
x_1	0.194	0.294
x_2	0.420491	0.435
y_1	0.411	0.511
y_2	-0.035	-0.035
T	31.3	50
I_{bat}	0.828	0.2
K_p	998.142273	0.8232
K_i	1001.14133	1.4551
K_d	1000.317279	0.1111
R_a	0.2053	0.1
J_a	0.4843	0.5

In the PID controller subsystem, the parameters are assumed constant. In the system integration, the parameters fixed in the subsystem are functions of the design variables in the other subsystems, as discussed earlier. The following four graphs show the responses of speed and subsystem objective value with time before and after integration.

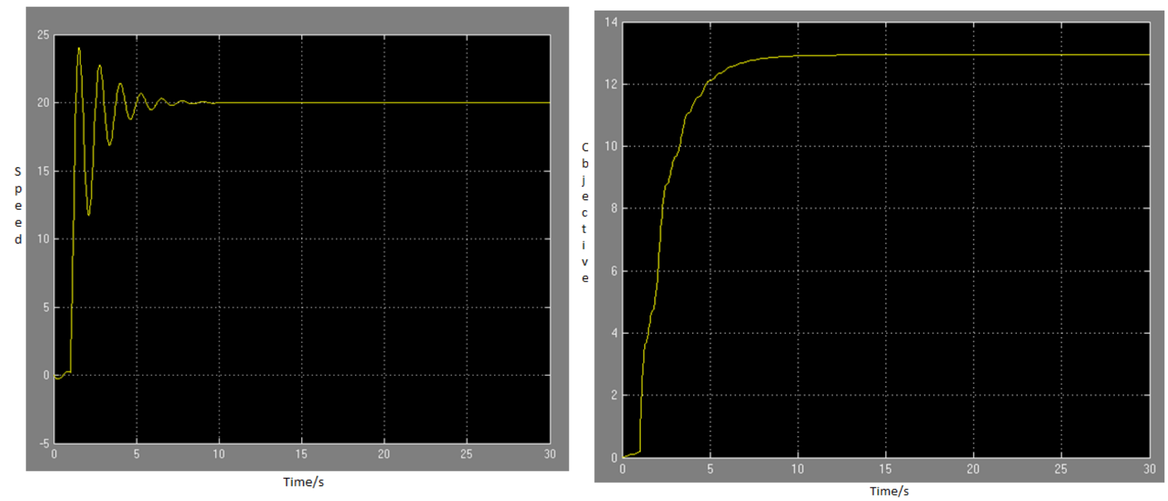

Figure 3.5.1: Responses of speed and subsystem objective value with time before integration

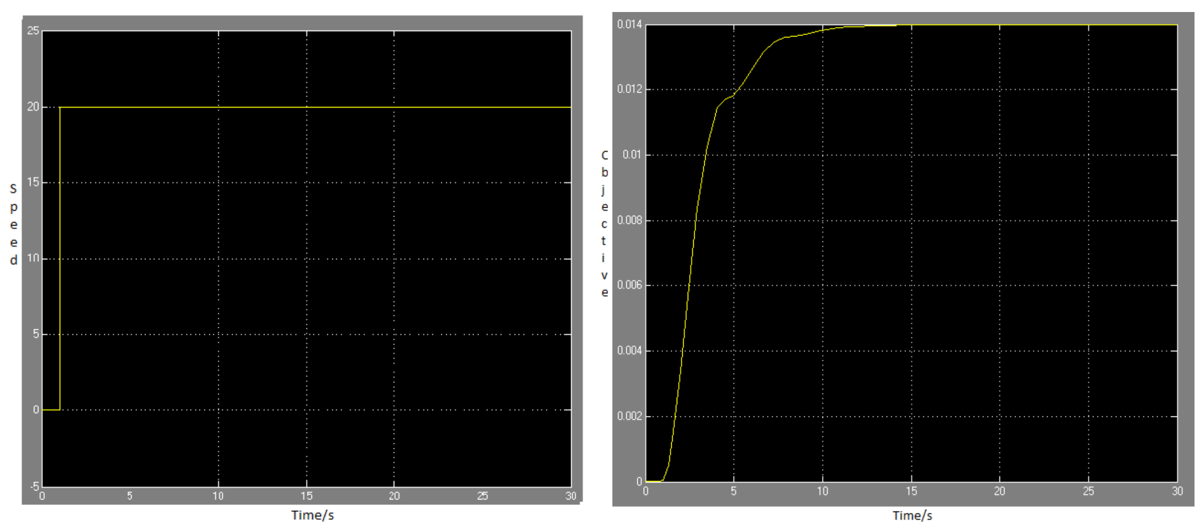

Figure 3.5.2: Responses of speed and subsystem objective value with time after integration

Table 3.5.2: Highlighted optimal solutions for controller subsystem

Status	Kp	Ki	Kd
Before integration	0.8232	1.4551	0.1111
After integration	998.1423	1001.1413	1000.3173

Table 3.5.3: Objective values and constraints for controller subsystem

Status	Objective value	Max overshoot	Settling time
Before integration	13.0275	23.84%	4.63s
After integration	0.0140	0	1.00s

From the comparisons, the optimal results are better than those from the subsystem without integration. One possible reason is that the parameters used in subsystem optimization are fixed and far from the optimal solution for this parameters in whole system. So the better solution is for the different values used for the parameters, which are design variables in integration.

The new solution is still too ideal for a practical application. The responses are perfect for a controller, which is hard to realize the exactly same response in real life. This makes sense for a theoretical PID controller in computer, but we can consider more real PID controller circuit in the future development.

For the battery subsystem, the optimization results are n = 3.66, I = 0.2, and T=50. Since n should be an integer in real case, it has been determined to be 4. For the integrated system, the optimization results of the variables from battery are n=3.22, I= 0.828, and T = 31.3. Also in this case, the optimal result for number of cells was modified to 4.

At first, some parts of objective of the battery subsystem become constraints for the integrated system. In the battery subsystem, it is formulated to maximize the battery cell's energy efficiency and capacity; while in the integrated system, boundaries were set for them in order to get reasonable optimal results. In the sub problem, to maximize the energy efficiency and battery capacity, it has been determined that low current and high temperature is required. Furthermore, the output voltage, which is a function of battery current, temperature, and number of cells, is a linking variable for the controller subsystem. The constraints in the controller subsystem will have an effect on the output voltage, and hence change the optimal values of battery's design variables. On the other hand, the battery's weight is a linking variable for the structure subsystem, which can lead to different optimal results. The objective and constraints were changed, and hence it is reasonable to get different optimal solutions.

ACKNOWLEDGEMENTS

We would like to thank Prof. Panos Y. Papalambros, Ms. Abigail Mechtenberg and Ms. Diane Peters from University of Michigan Ann Arbor for their help and input to this project.

REFERENCES

A. Muetze and Y.C. Tan, “Modeling and Analysis of the Technical Performance of DC-Motor Electric Bicycle Drives Based on Bicycle Road Test Data,” 1-4244-0743-5/07, 2007, IEEE

Annette Muetze, Ying Chin Tan, 2007, “Modeling and Analysis of the Technical Performance of DC-Motor Electric Bicycle Drives Based on Bicycle Road Test Data”, IEEE

D. Arola, P.G. Reinhall, M.G. Jenkins and S.C. Iverson, An Experimental Analysis Of a Hybrid Bicycle Frame, 1999

G.H. Kim and A. Pesaran, Battery thermal management system design modeling, Golden, Colo. : National Renewable Energy Laboratory, 2006

Henk Jan Bergveld, Wanda S. Kruijt and Peter H.L. Notten, battery management systems, design by modeling, 2002

Julie A. Reyer, Panos Y. Papalambros, 2002, “Combined Optimal Design and Control With Application to an Electric DC Motor”, ASME, Journal of Mechanical Design.

Essam S. Hamdi, “Design of Small Electrical Machines”, 1994

Leslie Brown, Measuring bicycle frame sizes / bike fitting.2008, http://www.tenerife-training.net/Tenerife-News-Cycling-Blog/2008/04/learning-curve/measuring-bicycle-frame-sizes-bike-fitting/

Sheldonbrown, 2008, http://www.sheldonbrown.com/harris/surly-specs.html.

Wikipedia, http://en.wikipedia.org/wiki/Electric_bicycle

APPENDIX A. MATLAB Codes for Subsystems

A.1 Battery subsystem

MATLAB code for simplified Battery model

```
function [f]= fun(x)

f= 0.3*13/(3.6-0.1*(0.00000008*x^4 - 0.00001*x^3 + 0.0006*x^2 -
0.0101*x+0.2735))/((0.00000009*x^4 - 0.000002*x^3-0.0005*x^2
+0.0282*x+0.8861)*(1-0.1*(0.00000008*x^4 - 0.00001*x^3 + 0.0006*x^2 -
0.0101*x+0.2735)/3.6));
```

```
function [g,h]= nonlcon (x)
g=[ x-50;
    10- x;
    0.00000009*x^4 - 0.000002*x^3-0.0005*x^2 +0.0282*x+0.8861-1.5;
    1.1-(0.00000009*x^4 - 0.000002*x^3-0.0005*x^2 +0.0282*x+0.8861);
    (0.00000009*x^4 - 0.000002*x^3-0.0005*x^2 +0.0282*x+0.8861)*13-40*(3.6-
0.1*(0.00000008*x^4 - 0.00001*x^3 + 0.0006*x^2 - 0.0181*x+0.2735));
    1.1*(3.6-0.1*(0.00000008*x^4 - 0.00001*x^3 + 0.0006*x^2 -
0.0181*x+0.2735))-(0.00000009*x^4 - 0.000002*x^3-0.0005*x^2
+0.0282*x+0.8861)*13;
    13-15*(3.6-0.1*(0.00000008*x^4 - 0.00001*x^3 + 0.0006*x^2 -
0.0181*x+0.2735))];
h=[];
```

```
clear all;
A=[];
b=[];
Aeq=[];
beq=[];
lb=[];
ub=[];
options=optimset('Algorithm','sqp');
xopt= fmincon('fun',30,A,b,Aeq,beq,lb,ub,'nonlcon',options)
```

A.2 DC-motor subsystem

Model with detailed parameters

```
A=[ ]; b=[ ]; Aeq=[ ]; beq=[ ]; % matrix/vectors for defining linear
constraints (not used)
lb = [0,0,0,0,0]; % lower bounds on the problem
ub = [ ]; % upper bounds on the problem
x0=[10,100,20,100,100]; % Initial starting point
options=optimset('Algorithm','interior-point');
[xopt,fval,exitflag,ouput,lambda] =
fmincon('FUN',x0,A,b,Aeq,beq,lb,ub,'NONLCON',options);


function [f]=FUN(x)
% Target function
f=0.0178*x(1)+0.0089*x(2)+24818.58*x(3)*(x(4)+x(5))^2;


function [g,h]=NONLCON(x)
% Inequality constraints
g=[-x(1);
    -x(2);
    -x(3);
    -x(4);
    -x(5);
    x(4)-0.241916;
    x(3)-1.413717*x(4);
    0.942478*x(4)-x(3);
    x(5)-0.2142857*x(4);
    -x(5)+0.1*x(4);
    x(5)-0.278431*x(4);
    x(5)-0.5*x(4);
    x(1)-9565.446*x(3)*x(4)-17279.17*(x(4)^2)-23913.62*x(5)*x(4);
    -x(1)+2869.634*x(3)*x(4)+5183.752*(x(4)^2)+7174.085*x(5)*x(4);
    x(1)-(2617994*x(3)+4729185*x(4)+6544985*x(5))*(x(4)-x(5))*x(5);
    18.715*(x(3)^3)+5.895*(x(3)^2)+0.606*x(3)+0.02-(x(3)^3)*x(2);
    -93.574*(x(3)^3)-29.476*(x(3)^2)-3.032*x(3)-1.029+(x(3)^3)*x(2);];
% Equality constraints
h=[ ];
```

Model for parametric study

```
clear all

% Parameters
global a
global Awa
global Awf
global bfc
global fcf
global nd
```

```
global p
global Pmind
global S
global yeta;
global rho
global rho_cu
global rho_fe
global fi

a=5;
Awa=2*10^(-6);
Awf=10^(-6);
bfc=0.045;
fcf=0.65;
nd=24;
p=2;
Pmind=0.67*(1-0.1);
S=10;
yeta=0.85;
rho=1.68*10^(-8);
rho_cu=8900;
rho_fe=7900;
fi=0.66;


A=[ ]; b=[ ]; Aeq=[ ]; beq=[ ]; % matrix/vectors for defining linear
constraints (not used)
lb = [0,0,0,0,0]; % lower bounds on the problem
ub = [ ]; % upper bounds on the problem
x0=[14,452,0.0546,0.0386,0.00386]; % Initial starting point
options=optimset('Algorithm','sqp');
[xopt,fval,exitflag,ouput,lambda] =
fmincon('FUN',x0,A,b,Aeq,beq,lb,ub,'NONLCON',options);


function [f]=FUN(x)

a=5;
Awa=2*10^(-6);
Awf=10^(-6);
bfc=0.045;
fcf=0.65;
nd=24;
p=2;
Pmind=0.67*(1-0.1);
S=10;
yeta=0.85;
rho=1.68*10^(-8);
rho_cu=8900;
rho_fe=7900;
fi=0.66;

% Target function
f=rho_cu*(Awa*x(1)+Awf*x(2))+rho_fe*x(3)*pi*(x(4)+x(5))^2;
```

```
function [g,h]=NONLCON(x)

a=5;
Awa=2*10^(-6);
Awf=10^(-6);
bfc=0.045;
fcf=0.65;
nd=24;
p=2;
Pmind=0.67*(1-0.1);
S=10;
yeta=0.85;
rho=1.68*10^(-8);
rho_cu=8900;
rho_fe=7900;
fi=0.66;

% Intermediate variables
ac=2*Pmind*x(1)/(pi*yeta*a*nd*(2*x(3)+2.3*pi*x(4)/p+5*x(5))*x(4));
hf=0.076*fi/x(3);
Lmtf=x(3)+2*bfc;
If=Awf*Awf*nd/(hf*Lmtf*bfc*fcf*p*rho);

% Inequality constraints
g=[-x(1);
    -x(2);
    -x(3);
    -x(4);
    -x(5);
    pi/p*x(4)-0.38;
    p*x(3)-0.9*pi*x(4);
    0.6*pi*x(4)-p*x(3);
    2*x(4)-3.5*(x(4)-2*x(5));
    2.5*(x(4)-2*x(5))-2*x(4);
    S*x(5)-2*pi*(x(4)-2*x(5));
    x(5)-0.5*x(4);
    ac-20;
    6-ac;
    1.2*x(1)*Awa-(2*x(3)+2.3*pi/p*x(4))*pi*(x(4)-x(5))*x(5);
    150*Awf*(Lmtf+bfc)*hf-100*If*If*x(2)*rho;
    100*If*If*x(2)*rho-750*Awf*(Lmtf+bfc)*hf;];
% Equality constraints
h=[ ];
```

A.3 Motor controller subsystem

```
%ME 555 project PID controller design
%Main steps
global Kp; %globalize the design varibal Kp in PID controller
global Ki; %globalize the design varibal Ki in PID controller
global Kd; %globalize the design varibal Kd in PID controller
global Kt; %globalize the design parameter torque constant Kt
global Kv; %globalize the design parameter back-emf constant Kv
global Ra; %globalize the design parameter armature resistance Ra
global La; %globalize the design parameter armature inductance La
global B;  %globalize the design parameter rolling resistance B
global J;  %globalize the design parameter inertia J
global Tload; %globalize the design parameter load torque Tload
global W0; %globalize the design parameter referance speed W0
x0=[0.823, 1.455, 0.2111]; %initial guess
Kt=5; % give parameters values
Kv=0.3;
Ra=0.1;
La=0.5;
B=0.01;
J=0.5;
Tload=1;
W0=20;
options=optimset('Algorithm','sqp');
A=[];b=[];Aeq=[];beq=[];
lb=[0,0,0];
ub=[];
[xopt,fval,exitflag,output,lambda,grad,hessian]=
fmincon('FUN',x0,A,b,Aeq,beq,lb,ub,'NONLCON',options)
```

FUN.m

```
function [f]=FUN(x)
%objective function
Kp=x(1);
Ki=x(2);
Kd=x(3);
% run simulation in simulink
%try
SimOut=sim('new_controller');
% the integral of the error between the reference and output speed.
f=max(objective);
```

NONLCON.m

```
function [g, h]= NONLCON (x)
global Kp; %globalize the design varibal Kp in PID controller
global Ki; %globalize the design varibal Ki in PID controller
global Kd; %globalize the design varibal Kd in PID controller
global Kt; %globalize the design parameter torque constant Kt
global Kv; %globalize the design parameter back-emf constant Kv
global Ra; %globalize the design parameter armature resistance Ra
global La; %globalize the design parameter armature inductance La
global B;  %globalize the design parameter rolling resistance B
```

```matlab
global J;  %globalize the design parameter inertia J
global Tload; %globalize the design parameter load torque Tload
global W0; %globalize the design parameter referance speed W0
Kt=5; % give parameters values
Kv=0.5;
Ra=0.1;
La=0.5;
B=0.01;
J=0.5;
Tload=1;
W0=20;
% Run simulation in simulink
Kp=x(1);
Ki=x(2);
Kd=x(3);
SimOut=sim('new_controller');
%Define maxovershoot
maxovershoot= (max(speed)- W0)/W0;
%Set upperlimit and lowerlimit
upperlimit=W0+W0*0.03;
lowerlimit=W0-W0*0.03;
%Find settling time
n=length(SimOut);
flag=0;
i=n;
while flag==0;
    if speed(i)<=upperlimit && speed(i)>=lowerlimit
        flag=0;
        i=i-1;
    else
        flag=1;
        settlingtime=SimOut(i);
    end
end
%inequality constraints
g=[maxovershoot-0.35;
    W0-maxovershoot;
    settlingtime-5;
    -settlingtime];
% eauality constraints
h=[];
```

A.4: Structure subsystem

Target Cell (Min)

Cell	Name	Original Value	Final Value
J1	f	4.96	3.86

Adjustable Cells

Cell	Name	Original Value	Final Value
D1	x1	0.244	0.294
D2	y1	0.4611	0.511
D3	x2	0.404	0.43538655
D4	y2	-0.039	-0.035
D7	D1	0.045	0.04
D8	d1	0.043	0.039
D9	D2	0.045	0.045997376
D10	d2	0.043	0.044091376

Constraints

Cell	Name	Cell Value	Formula	Status	Slack
B13	g1	0	B13<=0	Binding	0
B14	g2	2.32484E-07	B14<=0	Binding	0
B15	g3	-0.01	B15<=0	Not Binding	0.01
B16	g4	0	B16<=0	Binding	0
B17	g5	-0.004002624	B17<=0	Not Binding	0.004002624
B18	g6	-0.005997376	B18<=0	Not Binding	0.005997376
B19	g7	0	B19<=0	Binding	0
B20	g8	-0.009	B20<=0	Not Binding	0.009
B21	g9	-0.000905999	B21<=0	Not Binding	0.000905999
B22	g10	-0.008094001	B22<=0	Not Binding	0.008094001
B23	g11	-0.064009004	B23<=0	Not Binding	0.064009004
B24	g12	-0.010460349	B24<=0	Not Binding	0.010460349

B25	g13	-0.139539651	B25<=0	Not Binding	0.139539651
B26	g14	-0.035990996	B26<=0	Not Binding	0.035990996
B27	g15	-0.1	B27<=0	Not Binding	0.1
B28	g16	0	B28<=0	Binding	0
B29	g17	-0.1	B29<=0	Not Binding	0.1
B30	g18	0	B30<=0	Binding	0
B31	g19	-0.07138655	B31<=0	Not Binding	0.07138655
B32	g20	-0.00861345	B32<=0	Not Binding	0.00861345
B33	g21	-0.008	B33<=0	Not Binding	0.008
B34	g22	0	B34<=0	Binding	0
B33	g21	-0.008	B33<=0	Not Binding	0.008
B34	g22	0	B34<=0	Binding	0
B35	g23	-5555.827017	B35<=0	Not Binding	5555.827017
B36	g24	-17503.3391	B36<=0	Not Binding	17503.3391

Adjustable Cells

Cell	Name	Final Value	Reduced Gradient
D1	x1	0.294	0
D2	y1	0.511	0
D3	x2	0.43538655	0
D4	y2	-0.035	0
D7	D1	0.04	0
D8	d1	0.039	0
D9	D2	0.045997376	0
D10	d2	0.044091376	0

Constraints

Cell	Name	Final Value	Lagrange Multiplier
B13	g1	0	0.00569164

B14	g2	2.32484E-07	0.0030896
B15	g3	-0.01	0
B16	g4	0	0.00116927
B17	g5	-0.004002624	0
B18	g6	-0.005997376	0
B19	g7	0	0.045601686
B20	g8	-0.009	0
B21	g9	-0.000905999	0
B22	g10	-0.008094001	0
B23	g11	-0.064009004	0
B24	g12	-0.010460349	0
B25	g13	-0.139539651	0
B26	g14	-0.035990996	0
B27	g15	-0.1	0
B28	g16	0	5.13189E-06
B29	g17	-0.1	0
B30	g18	0	0.00027137
B31	g19	-0.07138655	0
B32	g20	-0.00861345	0
B33	g21	-0.008	0
B34	g22	0	0.000178792
B35	g23	-5555.827017	0
B36	g24	-17503.3391	0

```
A=[ ]; b=[ ]; Aeq=[ ]; beq=[ ]; % matrix/vectors for defining linear
constraints (not used)
lb = [ ]; % lower bounds on the problem
ub = [ ]; % upper bounds on the problem
m0=[0.045,0.043,0.244,0.461,0.045,0.043,0404,-0.039]; % Initial starting
point
options=optimset('Algorithm','interior-point');
[mopt,fval,exitflag,ouput,lambda] =
fmincon('FUN2',m0,A,b,Aeq,beq,lb,ub,'NONLCON2',options);


function [f]=FUN2(m)
```

```
% the percent sign allows me to write in comments
f = 7.853*(m(1)^2-m(2)^2)*((m(3)^2 + m(4)^2))^0.5+(m(5)^2-m(6)^2)*(((m(3)-
m(7))^2 + (m(4)-m(8))^2))^0.5;


function [g,h]=NONLCON2(m)
% Inequality constraints
l1=((m(3)^2 + m(4)^2))^0.5;
l2=(((m(3)-m(7))^2 + (m(4)-m(8))^2))^0.5;

g=[
    4*900*((m(7)-m(3))*m(3)/(l2*m(4))+(m(4)-m(8))/l2)^(-1)*((m(7)-
m(3))/l2*m(3)/l1)-6*301415*(m(1)^2-m(2)^2);
    4*900*((m(7)-m(3))*m(3)/(l2*m(4))+(m(4)-m(8))/l2)^(-1)-6*301415*(m(5)^2-
m(6)^2);
    m(1)-0.05;
    -m(1)+0.04;
    m(5)-0.05;
    -m(5)+0.04;
    m(2)-m(1)+0.001;
    m(1)-m(2)-0.01;
    m(6)-m(5)+0.001;
    m(5)-m(6)-0.01;
    0.5-l2;
    l1-0.6;
    0.45-l1;
    l2-0.6;
    0.194-m(3);
    m(3)-0.294;
    0.411-m(4);
    m(4)-0.511;
    0.364-m(7);
    m(7)-0.444;
    -0.043-m(8);
    m(8)+0.035;
   ];
% Equality constraints
h=[ ];
```

APPEDNDIX B. MATLAB Codes for integrated system

```
function [f]=FUN(x)
global Kp; %globalize the design varibal Kp in PID controller
global Ki; %globalize the design varibal Ki in PID controller
global Kd; %globalize the design varibal Kd in PID controller
global Kt; %globalize the design parameter torque constant Kt
global Kv; %globalize the design parameter back-emf constant Kv
global Ra; %globalize the design parameter armature resistance Ra
global La; %globalize the design parameter armature inductance La
global B;  %globalize the design parameter rolling resistance B
global J;  %globalize the design parameter inertia J
global Tload; %globalize the design parameter load torque Tload
global W0; %globalize the design parameter referance speed W0
Kt=5; % give parameters values
Kv=0.5;
%Ra=0.1;
La=0.5;
B=0.01;
%J=0.5;
Tload=1;
W0=20;
% Target function
f=0.0178*x(1)+0.0089*x(2)+24818.58*x(3)*(x(4)+x(5))^2+0.3*x(6)+2120*((x(7)^2-
x(9)^2)*(x(11)^2+x(13)^2)^0.5+(x(8)^2-x(10)^2)*((x(11)-x(12))^2+(x(13)-
x(14))^2)^0.5);

function [g,h]=NONLCON1(x)
global Kp; %globalize the design varibal Kp in PID controller
global Ki; %globalize the design varibal Ki in PID controller
global Kd; %globalize the design varibal Kd in PID controller
global Kt; %globalize the design parameter torque constant Kt
global Kv; %globalize the design parameter back-emf constant Kv
global Ra; %globalize the design parameter armature resistance Ra
global La; %globalize the design parameter armature inductance La
global B;  %globalize the design parameter rolling resistance B
global J;  %globalize the design parameter inertia J
global Tload; %globalize the design parameter load torque Tload
global W0; %globalize the design parameter referance speed W0
Kt=5; % give parameters values
Kv=0.5;
%Ra=0.1;
La=0.5;
B=0.01;
%J=0.5;
Tload=1;
W0=20;

Kp=x(17);
Ki=x(18);
Kd=x(19);

% Run simulation in simulink
SimOut=sim('new_controller');
```

```
%Define maxovershoot
maxovershoot= (max(speed)- W0)/W0;
%Set upperlimit and lowerlimit
upperlimit=W0+W0*0.03;
lowerlimit=W0-W0*0.03;
%Find settling time
n=length(SimOut);
flag=0;
i=n;
while flag==0;
    if speed(i)<=upperlimit && speed(i)>=lowerlimit
        flag=0;
        i=i-1;
    else
        flag=1;
        settlingtime=SimOut(i);
    end
end
% Inequality constraints
g=[-x(1);%g1
    -x(2);%g2
    -x(3);%g3
    -x(4);%g4
    -x(5);%g5
    x(4)-0.241916;%g6
    x(3)-1.413717*x(4);%g7
    0.942478*x(4)-x(3);%g8
    x(5)-0.2142857*x(4);%g9
    -x(5)+0.1*x(4);%g10
    x(5)-0.278431*x(4);%g11
    x(5)-0.5*x(4);%g12
    x(1)-9565.446*x(3)*x(4)-17279.17*(x(4)^2)-23913.62*x(5)*x(4);%g13
    -x(1)+2869.634*x(3)*x(4)+5183.752*(x(4)^2)+7174.085*x(5)*x(4);%g14
    x(1)-(2617994*x(3)+4729185*x(4)+6544985*x(5))*(x(4)-x(5))*x(5);%g15
    18.715*(x(3)^3)+5.895*(x(3)^2)+0.606*x(3)+0.02-(x(3)^3)*x(2);%g16
    -93.574*(x(3)^3)-29.476*(x(3)^2)-3.032*x(3)-1.029+(x(3)^3)*x(2);%g17
    x(15)-50;%g18
    10-x(15);%g19
    x(16)-10;%g20
    0.1-x(16);%g21
    13-x(6)*(3.6-x(16)*(8*10^(-8)*x(15)^4-10^(-5)*x(15)^3+0.0006*x(16)^2-
0.0181*x(15)+0.2735));%g22
    x(6)*(3.6-x(16)*(8*10^(-8)*x(15)^4-10^(-5)*x(15)^3+0.0006*x(16)^2-
0.0181*x(15)+0.2735))-50;%g23
    0.00000009*x(15)^4-0.000002*x(15)^3-0.0005*x(15)^2+0.0282*x(15)-
0.6139;%g24
    0.2139-(0.00000009*x(15)^4-0.000002*x(15)^3-
0.0005*x(15)^2+0.0282*x(15));%g25
    (0.00000009*x(15)^4-0.000002*x(15)^3-
0.0005*x(15)^2+0.0282*x(15)+0.8861)*x(6)-40;%g26
    1.1-(0.00000009*x(15)^4-0.000002*x(15)^3-
0.0005*x(15)^2+0.0282*x(15)+0.8861)*x(6);%g27
    x(6)-15;%g28
    -x(6);%g29
    4*(2.94*x(6)+900)*x(13)*(x(12)-x(11))*(x(11)^2+x(13)^2)^0.5-
18.85*1000000*(x(7)^2-x(9)^2)*(x(13)-x(14));%g30
```

```
    4*(2.94*x(6)+900)*x(13)*(x(12)-x(11))*((x(11)-x(12))^2+((x(13)-
x(14))^2)^0.5-18.85*1000000*(x(8)^2-x(10)^2)*(x(11)*x(12)-x(11)^2)*(x(13)-
x(14)));%g31
    x(7)-0.05;%g32
    -x(7)+0.04;%g33
    x(8)-0.05;%g34
    -x(8)+0.04;%g35
    x(9)-x(7)+0.001;%g36
    x(7)-x(9)-0.01;%g37
    x(10)-x(8)+0.001;%g38
    -x(10)+x(8)-0.01;%g39
    0.25-(x(11)-x(12))^2-(x(13)-x(14))^2;%g40
    x(11)^2+x(13)^2-0.36;%g41
    -(x(11)^2+x(13)^2)+0.2025;%g42
    (x(11)-x(12))^2+(x(13)-x(14))^2-0.36;%g43
    0.194-x(11);%g44
    x(11)-0.294;%g45
    0.411-x(13);%g46
    x(13)-0.511;%g47
    0.364-x(12);%g48
    x(12)-0.444;%g49
    -0.043-x(14);%g50
    x(14)+0.035;%g51
    maxovershoot-0.35;%g52
    W0-maxovershoot;%g53
    settlingtime-5;%g54
    -settlingtime;%g55
    x(16)*(0.00000009*x(15)^4-0.000002*x(15)^3-
0.0005*x(15)^2+0.0282*x(15)+0.8861)-1.08;%g56
    -x(16)*(0.00000009*x(15)^4-0.000002*x(15)^3-
0.0005*x(15)^2+0.0282*x(15)+0.8861);%g57
    ];
% Equality constraints
h=[Ra-0.0021*x(1);
    J-(12409.3*x(3)*(0.5*x(4)-x(5))^2-0.0089*x(1)*(x(4)-x(5))*x(5))];


A=[ ]; b=[ ]; Aeq=[ ]; beq=[ ]; % matrix/vectors for defining linear
constraints (not used)
lb = [0,0,0,0,0,0,0,0,0,0,0,0,0,-1,0,0]; % lower bounds on the problem
ub = [ ]; % upper bounds on the problem
x0=[10,200,0.1,0.1,0.01,4,0.045,0.045,0.043,0.043,0.244,0.461,0.404,-
0.037,31,0.5,1000,1000,1000]; % Initial starting point
options=optimset('Algorithm','sqp','TolX',0.00001);
global Kp; %globalize the design varibal Kp in PID controller
global Ki; %globalize the design varibal Ki in PID controller
global Kd; %globalize the design varibal Kd in PID controller
global Kt; %globalize the design parameter torque constant Kt
global Kv; %globalize the design parameter back-emf constant Kv
global Ra; %globalize the design parameter armature resistance Ra
global La; %globalize the design parameter armature inductance La
global B;  %globalize the design parameter rolling resistance B
global J;  %globalize the design parameter inertia J
global Tload; %globalize the design parameter load torque Tload
global W0; %globalize the design parameter referance speed W0
Kt=5; % give parameters values
```

```
Kv=0.5;
%Ra=0.1;
La=0.5;
B=0.01;
%J=0.5;
Tload=1;
W0=20;
[xopt,fval,exitflag,ouput,lambda] =
fmincon('FUN',x0,A,b,Aeq,beq,lb,ub,'NONLCON1',options);
```